J. theor. Biol. (1994) **167**, 323–360

Mathematical Model of Antiviral Immune Response III. Influenza A Virus Infection

G. A. BOCHAROV AND A. A. ROMANYUKHA

Institute of Numerical Mathematics, Russian Academy of Sciences, Leninskij Prospekt 32-*A*, 117334 *Moscow, Russia*

(*Received on* 4 *December* 1992, *Accepted on* 26 *August* 1993)

We present an approach to studying theoretically the regularities and the kinetic characteristics of influenza A virus (IAV) infection in man. The estimates of the "numbers" (Zinkernagel *et al.*, 1985) characterizing evolutionary established interferon and immune responses in uncomplicated IAV infection are explored by developing a multiparameter mathematical model which allows direct quantitative references to the biological reality. The system of equations of the mathematical model of antiviral immune response, applied earlier to acute hepatitis B virus infection (Marchuk *et al.*, 1991*a*, *b*), is modified and extended to describe the joint reaction of the interferon and immune systems in IAV infection. Macrophages infiltrating the airway's epithelium are considered to be the principal source of interferon that induces antiviral resistance in lung epithelial cells. The model is formulated as a delay-differential system with about 60 parameters characterizing the rates of various processes contributing to the typical course of IAV infection. The key aspect of the adjustment between the model and various data on the immunity to influenza is the derivation of a consistent data set—the generalized picture of uncomplicated IAV infection. It serves as a consistent theoretical definition of the structure of the normal course of the infection and the antiviral immune response suitable for model fitting. The parameter estimates for the processes considered in the model are carefully discussed. The quantitative model is used to study the organization and dynamic properties of the processes contributing to IAV infection. The threshold condition for immune protection of virus-free host to infection with IAV is analyzed. The relative roles of humoral, cellular and interferon reactions for the kinetics of the uncomplicated IAV infection are studied. The contribution of parameters of virus—sensitive tissue, interferon and IAV-specific immune processes to the variations of duration and severity of the infection is quantitatively estimated by sensitivity studies. It is shown that the variations in the parameters of a virus–epithelial cell system are more influential on the severity of the infection rather than that of the antiviral immune response. The need for fine co-ordination of the kinetics of the non-specific interferon response and the adaptive antigen-specific immune reactions to provide recovery from the infection is illustrated.

1. Introduction

One of the clearly established functions of an immune system is to protect a host against various infectious agents. Recovery from infectious diseases caused by viruses can be viewed as resulting from the balance between two processes: the ability of viruses to infect and destroy sensitive tissue cells and the ability of the immune and non-specific defense systems to limit the spread of the infectious agent, to neutralize free viruses and to kill infected cells in order to prevent further virus replication. Some viruses, like influenza A virus (IAV), are highly cytopathic and therefore threaten the life of their host much more than weakly cytopathic viruses, like hepatitis B virus (HBV). The more destructive for sensitive tissue cells a virus is, the greater is the need for rapid and efficient elimination by the host's immune systems. However, such an efficient approach may have disadvantages when dealing with weakly cytopathic viruses: these may cause

0022–5193/94/080323 + 38 $8.00/0

immunologically mediated damage of cells and organs, as in the case of chronic active hepatitis B (Zinkernagel *et al.*, 1985).

Both the course and the outcome of any infectious disease are influenced on the one hand by virus cytopathogenicity, tissue tropism, rapidity of spread, generation time, susceptibility to interferon (IFN), etc, and on the other hand by the host's degree of immunocompetence, MHC-linked Ir-gene dependent immunoresponsiveness, non-specific defense systems, etc, (Zinkernagel *et al.*, 1985). There is a need to assess these factors in quantitative terms to provide a firm basis for further rigorous analysis of host immunity to virus infections (Doherty, 1985, 1986; Zinkernagel *et al.*, 1985). Consequently, one purpose of our modeling was to estimate parameters governing the "normal" course of influenza infection. In addition, the complexity of the human immune system is so high that predictive understanding of the mechanisms of infectious diseases can not be achieved without careful mathematical modeling. In this paper we develop a mathematical model for specific and non-specific (IFN) components of the immune responses in IAV infection with a complexity appropriate to the level of current knowledge of the IAV infection mechanisms.

It is accepted in immunology that the major problem in understanding the nature of immunity is related to the difficulty of dealing conceptually with the complexity of the immune system *in vivo* (Doherty, 1985, 1986; Zinkernagel *et al.*, 1985; Paul, 1987). This is confirmed by intensive recent theoretical research (Perelson, 1988; Segel & Perelson, 1989; Stewart & Varela, 1990; Weisbuch, 1990; De Boer & Perelson, 1991; Perelson & Weisbuch, 1992; De Boer *et al.*, 1992*a*, *b*; Weisbuch *et al.*, 1992). The study of virus infections is one of the central aspects of experimental and clinical investigations of the immune response. There is, as yet, no quantitatively consistent view for most viral infections of the particular roles of the humoral and cellular components of the immune system, as well as other non-specific defense processes in the protection, recovery and pathology of the host. A theoretical approach based on mathematical modeling offers new opportunities for quantitative understanding of the organization and the kinetic regularities of the antiviral immune responses. In the mathematical model presented below, particular attention is paid to the analysis and representation of the kinetics of antigen-driven humoral and cellular reactions in IAV infection.

Influenza remains the major epidemic viral disease in man. Various aspects of the infection are clearly understood and well documented. It is a complex biological phenomenon with a wide spectrum of clinical outcomes. The quantitative influence of virus-related factors, specific immunity parameters as well as non-specific components of immune reactions (IFN, inflammation) on variations in the duration and severity of influenza infection need to be assessed for clinical practice. To this end a mathematical model quantitatively representing the major mechanisms of uncomplicated IAV infection is developed in the paper.

When foreign antigens such as viruses or bacteria are given to the immune system, then a cascade of defense processes including interferon system activation, lymphocyte proliferation and differentiation, inflammation, etc. occurs to protect the host. The magnitude of the host's antiviral responses depends on intercellular interactions in peripheral lymphoid tissues while the protective efficiency results from the "number games" (Zinkernagel *et al.*, 1985) between infectious agents and the defense systems. The estimates of the "numbers" characterizing evolutionary established immune and interferon responses in uncomplicated IAV infection are explored by deriving a multiparameter mathematical model, which allows direct quantitative references to the biological reality. Our research is intended to complement the current work of the experimental and theoretical immunologists.

Let us review briefly the principal processes of antiviral immunity which are common for viral infections (Doherty, 1985, 1986; Zinkernagel *et al.*, 1985; Ada & Jones, 1986). To initiate infection, viruses enter their host and infect the susceptible tissues. This results in viral replication and the production of cellular injury. The latter is the basis for clinical illness. All viruses give the immune system a signal, either on the surface of infected cells or on antigen-presenting cells. Macrophages play a central role in the induction and amplification of specific immune response. Both the cellular and humoral limbs of the immune system are activated during viral infections. Cellular immunity is represented mainly by cytotoxic T cells (CTLs) that act locally via contact on a one-to-one cell basis in solid tissue. The humoral immunity is composed of B cells, plasma cells and antibodies. Helper T cells play a crucial part in the generation of both CTLs and humoral immunity. Induction and triggering of the effector mechanisms of T cells depends on viral antigens being presented by macrophages of lymph nodes, or tissue macrophages in association with class I or class II MHC molecules. This facilitates interactions in lymphoid tissue, where most class II MHC positive cells are found, and the IL-2 and other factors secreted by

helper T cells operate at short range to promote lymphocyte proliferation and differentiation. Virus-specific CTLs, following clonal expansion and differentiation, enter the lymph and localize to tissue sites of virus replication where they deliver a lytic signal to virus-infected cells before infectious progeny are assembled and secreted.

It is accepted that CTLs are important in recovery from virus infection. The cytotoxic immunity displays a protective function by eliminating virus-producing cells, and a pathological effect, by destroying the host's virus-susceptible cells. Antibodies neutralize and remove virus particles from lymph, blood or other body fluids (mucosae). Protection against reinfection by the same viruses depends mostly on pre-existing levels of B cells and antibodies. The above short-range structure of the immune processes that are common for all acute viral infections including influenza is represented in a mathematical model of antiviral immune response (Marchuk *et al.*, 1991*a*). Besides, there are nonspecific mechanisms of defense that also contribute to the control of virus infections: the interferon system and inflammatory processes.

The aim of the present research is to develop a mathematical model quantitatively describing the typical kinetics of the antiviral immune response in uncomplicated IAV infection. The model considers the following components of antiviral immune responses: the antigen-specific cellular and humoral components and the interferon components. The integrative model of IAV infection is constructed in two steps. First, a model for specific antiviral immune responses is developed, making use of our previous experience in quantitative modeling of an acute HBV infection (Marchuk *et al.*, 1991*a*, *b*). Particular attention is paid to the description of the epithelial destruction in the lung, with the inflammation processes taken into account. HBV is a slowly replicating, poorly cytopathic virus, while IAV is rapidly replicating and highly cytopathic. An assessment of the quantitative parameters characterizing an immune response in the cases of both "slow" and "fast" viruses seems to be useful in elucidating the importance of the interferon response in limiting the spread of IAV at the initial stages of the infectious disease, before the immune defense is brought into play.

The second stage in developing a mathematical model of influenza A infection is related to derivation of a submodel for interferon system activation in the upper respiratory tract. Macrophages infiltrating the airway's epithelium are considered to be the principal source of the IFN that is responsible for establishing antiviral resistance in lung epithelial cells. Thereafter, the specific antiviral immune response and the interferon system models are combined to give an integrative representation for the kinetics of the principal processes of IAV infection. Thus, the infectious process is characterized by 13 time-dependent variables: viruses, antigen-presenting cells, Th1 cells, Th2 cells, CTLs, B cells, plasma cells, antibodies, virus-infected epithelial cells, IFN-protected epithelial cells, damaged epithelial cells, α-interferon and IFN-producing macrophages. The model is formulated as a delay-differential system with about 60 kinetic and homeostatic parameters characterizing the rates of various processes operating in the infection. The key aspect of the adjustment between the model and various data on the immunity to IAV infection is the derivation of a consistent data set, the generalized picture of uncomplicated influenza, which provides a theoretical definition of the structure of the typical course of disease and the normal antiviral immune response.

It seems important to explore the point that a realistic mathematical model of the infectious disease can be developed from a number of simpler submodels of contributory processes. The necessary corrections of the submodels should not destroy the core descriptive tools: data in the form of "generalized pictures", and particular sets of parameter values. The model developed in this paper provides a tool for knowledge organization by relating different particular factors and heterogeneous data from immunology, virology and clinical practice into an integrated and consistent quantitative description of the IAV infection, and a single scale for analysis and comparison of immune reactions during different infections (e.g. caused by HBV and IAV).

The organization of the paper is as follows. In Section 2 the nature of immunity to IAVs is reviewed. The construction of the generalized picture of IAV infection is presented in Section 3. In Section 4 the parameter estimation of the antiviral immune response model is developed. A number of parameter estimates are refined by fitting the antiviral immune response model to the generalized picture data for IAV infection. In Section 5 the model for interferon response is developed. The extended model for antiviral immune and interferon responses is used in Section 6 to make quantitative predictions concerning the factors responsible for protection against re-infection and variations in influenza course among individuals. The mathematical details of parameter fitting procedures are presented in the Appendix.

2. Nature of Immunity to Influenza A Virus Infection

Detailed reviews are now available concerning different aspects of influenza, both from the

immunological and the virological points of view (see Sweet & Smith, 1980; Couch & Kasel, 1983; Mitchell *et al.*, 1985; Murphy & Webster, 1985; Ada & Jones, 1986). They provide a solid conceptual basis for developing quantitative models of influenza in humans and are shortly summarized below.

Influenza viruses are divided into three types, A, B and C. Virus A is of great epidemiological danger, since its antigenic structure is continuously changing. The virus particles have two surface antigens, the hemagglutinin (HA) and the neuraminidase (NA). The HA is responsible for attachment and for penetration of the virus into cells. Both HA and NA are present on infected cell membranes. The virion contains also the envelope-associated matrix (M) protein and important internal proteins: nucleoprotein (NP) and polymerase (P). The antigenic variations in HA and NA are responsible for the epidemic potential of IAV. Antibodies to HA are strain-specific and neutralize the infectivity of the influenza A virus. Antibodies to NA have a less protective effect, while antibodies to the NP and M have no protective effect on the influenza A virus. Thus, it seems to be a reasonable simplification to associate the antigenic properties of influenza A virus with the HA determinant.

Human influenza is an infection of the upper respiratory tract and the major central airways. As the virus multiplies in the epithelium throughout the respiratory tract it causes degeneration and necrosis. The pathology, characterized by desquamation of the epithelium, involves the nasal mucosa, larynx and tracheobronchial tree. Complete resolution of epithelial necrosis probably takes up to a month. Infection with influenza A virus can result in a spectrum of clinical responses ranging from an asymptomatic infection to a primary viral pneumonia that rapidly progresses to a fatal outcome. The typical uncomplicated influenza syndrome is tracheobronchitis with the additional involvement of small airways (Murphy & Webster, 1985).

The incubation period ranges from 24 hr to 4 or 5 days depending on the dose of the virus and the immune status of the host. Non-specific components of the immune response to influenza virus (fever, interferon) are considered to have an important role in limiting viral spread and initiating recovery prior to the development of virus-specific T and B responses (see Fig. 1). Influenza viruses are sensitive to interferons. The IFNs secreted by macrophages induce a resistant state to virus infection in epithelial cells. The IFNs secreted by cytotoxic T cells have a lesser effect on inhibition of virus replication but increase target cell expression of MHC antigens and active NK cells

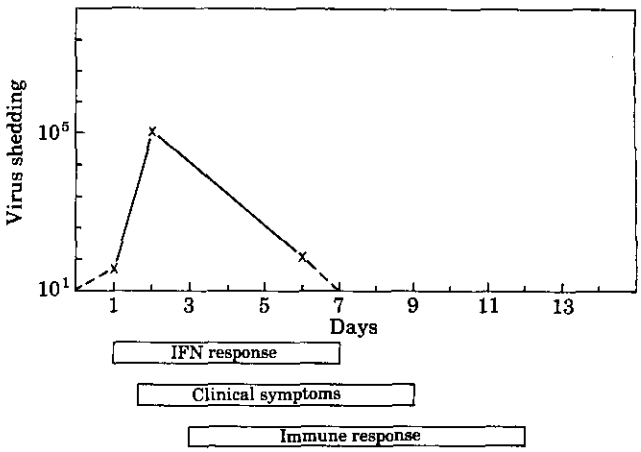

FIG. 1. Scheme of defense processes in influenza A virus infection. (Elaborated from Mitchell *et al.*, 1985; Murphy & Webster, 1985; Ada & Jones, 1986.)

which can mediate non-specific lysis of infected cells, thus acting as an amplification signal to enhance CTL-mediated destruction of virus-infected cells. Large numbers of macrophages may become activated and gain access to virus-infected cells at the mucosal surface participating in the inflammatory response to influenza infection. Delayed-type hypersensitivity T cells have been demonstrated to play a minor protective role during influenza infection but are considered to be a major component of the inflammatory process. Non-specific amplification of the specific CTL action seems to be extremely important for control of IAV infection. Information concerning the possible role of $\gamma\delta$T cells, located in airway walls, in limiting virus spread (Janeway, 1988), and late stages of IAV elimination (Born *et al.*, 1991) are contradictory, but both nonspecific effects may be described similarly to inflammatory processes (Janeway, 1992). Recovery from influenza infection involves specific humoral and cell-mediated immune responses, and conclusions regarding the relative importance of each are not possible at present. IAV-induced helper T cell clones, stimulated by virus antigens presented by macrophages in the context of MHC class II molecules, are both subtype-specific and cross-reactive. They may be specific for HA, NA, M and NP.

The induction of cytoxic T cells requires the presentation of viral antigens by macrophages or dendritic cells in the context of MHC class I molecules. CTLs are able to kill cells and destroy sensitive tissue by direct MHC-restricted cytotoxic effects on a cell-to-cell basis and/or recruitment of inflammatory cells. It was established that the most CTLs generated by IAV virus are cross-reactive, i.e. they react with determinants shared by all influenza A viruses, although

some distinguish between virus subtypes. CTL may be specific for HA, NP, P. HA-specific CTLs and Abs were shown to recognize different epitopes. It is important that most cases of influenza in adult humans may be considered to proceed in the context of a secondary CTL response. Natural influenza in humans induces T cell memory, with the half-life of CTL memory estimated to be 2–3 years.

B cell recognition is sensitive to variation in the antigenic structure of HA and NA. Antibodies to HA, to be protective, must be present at the mucosal surface—having been produced by plasma cells locally or derived from serum, i.e. by lymph nodes or blood plasma cells. The relative proportion of IgG to IgA increases in the lower part of respiratory tract. When virus is transmitted naturally by aerosol, it is deposited throughout the respiratory tract and locally produced antibodies, IgA, and possibly IgG, with an additional effect from serum-derived IgG, prevent infection (Ada & Jones, 1986). The presence of local Abs specific for HA induced by infection with attenuated virus correlated with resistance of humans to infection and illness after challenge with a virulent wild-type IAV (Murphy *et al.*, 1982). It has been also observed that there is a correlation between the level of serum HA-specific antibodies and resistance to infection or illness (Couch & Kasal, 1983). Suppressor T cells, which were subtype-specific, have been described but their precise role in recovery from influenza is not clear.

Virus-infected epithelial cells express on their membrane both HA-antigens and MHC class I molecules. The basic viral and immune processes of uncomplicated IAV infection take place in different organs and systems of the humans (Fig. 2). It is established that the virus–epithelial cells interactions are confined by the lung epithelium compartment (LE) of the upper and central parts of lung airways with diameter $>3{\cdot}3$ mm, having a volume $Q_{LE} \approx 0{\cdot}6$ ml (Weibel, 1986). Activation, proliferation and differentiation of immunocompetent cells are localized to lung associated lymphoid tissue (LALT) with the volume $Q_{LALT} \approx 12$ ml (Sapin & Borziak, 1982). The processes of CTL-mediated killing of infected cells and neutralization of IAVs by antibodies take place in the mucous space of the upper and central parts of lung airways, with a total volume $Q_M \approx 0{\cdot}4$ ml (Fedoseev & Geharev, 1989). Typical quantitative characteristics of the structure of human upper airways are presented in Tables 1 and 2.

To develop a mathematical model for uncomplicated IAV infection we represented the basic immune

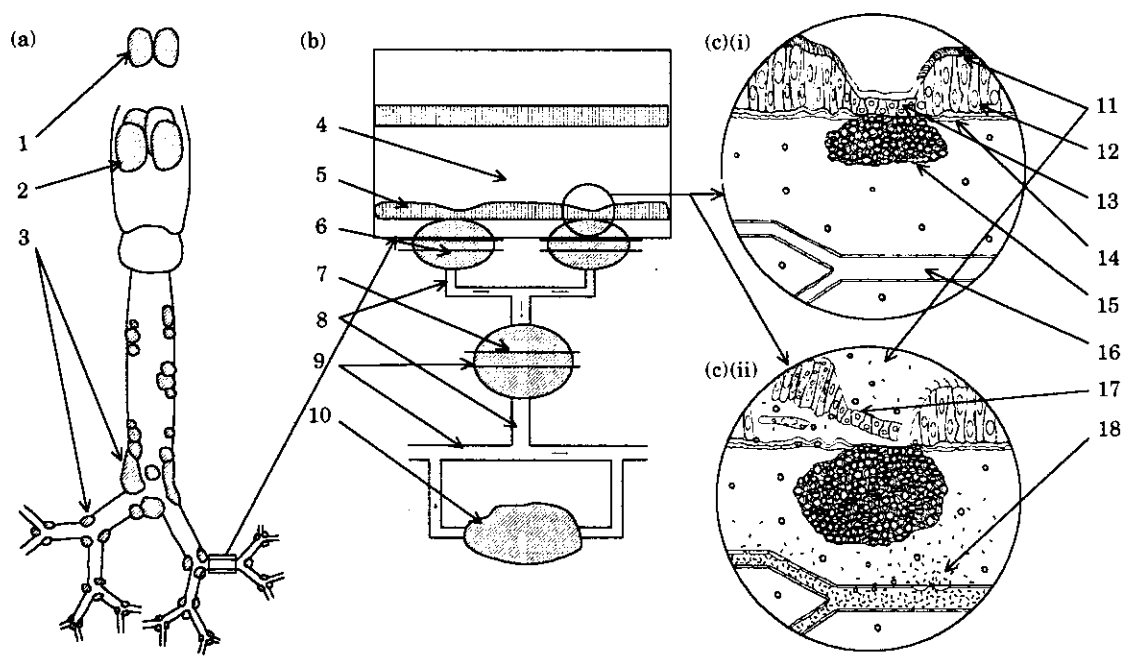

FIG. 2. The scheme of spatial organization of defense processes during viral infection of the human respiratory system. (a) Lung-associated lymphoid tissue (LALT). 1. adenoid; 2. tonsils; 3. bronchus-associated lymphoid tissue (BALT). (b) bronchi and BALT. 4. lumen of the bronchus; 5. ciliated epithelium; 6. lymphatic nodule; 7. lymph node; 8. lymphatic vessels; 9. blood vessels; 10. spleen. (c)(i) Normal state of bronchial wall. (c)(ii) Pathological state of bronchial wall. 11. mucus and fluid lining the airways; 12. ciliated epithelium; 13. lymphoepithelium; 14. basement membrane; 15. lymphatic nodule; 16. blood vessel; 17. virus-induced epithelium damage; 18. infiltration and exudation from capillary.

TABLE 1
Characteristics of structure of human upper airways

Name of characteristics	Value (unit)	References
Area of epithelium-covered six upper generations of respiratory tract	0·01–0·06 (m^2)	Weibel (1978) (estimate)
Thickness of epithelium layer (distance between bronchi lumen and basement membrane)	$5–7 \times 10^{-5}$ (m)	Heino *et al.* (1990)
Thickness of fluid lining the epithelium	$5–7 \times 10^{-6}$ (m)	Newhouse *et al.* (1976)
Part of internal bronchial surfaces occupated by ciliated cells	60–80%	Fedoseev *et al.* (1989) (estimate)
Percentage area of the intercellular spaces (of cross-sectional epithelial area):		
in normal condition	0·6%	Heino *et al.* (1990)
during inflammation	10%	Heino *et al.* (1990)
Percentage of lymphocytes in total inflammatory cells count (in cross-sectional epithelial area)	>90%	Heino *et al.* (1990)
Number of ciliated cells per mm^2 of cross-sectional epithelial area:		Heino *et al.* (1990)
in normal condition	2200 (cells)	
during inflammation	700 (cells)	
Number of inflammatory cells per mm^2 of cross-sectional epithelial area:		Heino *et al.* (1990)
in normal condition	200 (cells)	
during inflammation	1700 (cells)	
Area of the epithelial surface in one ciliated cell	$2–4 \times 10^{-11}$ (m^2)	Fedoseev *et al.* (1989) (estimate)
Percentage of macrophages (in total number of cells obtained by endobronchial lavage)	80–90%	Reynolds & Newball (1976)
Rate of macrophage removal from upper airways	10^6 (hr^{-1})	Brain (1970)

and viral processes of the infection by the following characteristics, having different localization:

- free influenza A viruses (V_f) able to infect epithelial cells (in the mucous compartment);
- infected (C_V) and destroyed epithelial cells (m) (within lung epithelium compartment);
- antigen-presenting macrophages (M_V), and IAV-specific helper T cells (H_E, H_B), cytotoxic T lymphocytes (E), B lymphocytes and plasma cells (B, P) (in the lymph nodes of LALT). The CTL population is considered in the model to be functionally uniform and is characterized by a single variable. We refer it to the lymph nodes of the LALT compartment and consider the concentration of mature CTLs in the mucous compartment to be proportional to that in lymph nodes.

TABLE 2
Estimated characteristics of human upper airways structure (Elaborated using the Table 1 data)

Name of characteristics	Value (unit)
Total number of ciliated cells lining six upper branches of airways	
in normal condition	$2 \times 10^8–3 \times 10^9$
during inflammation	$7 \times 10^8–10^9$
Total number of leukocytes distributed in epithelium layer covering six upper branches of airways	
in normal condition	$2 \times 10^7–3 \times 10^8$
during inflammation	$10^8–2 \times 10^9$
Volume of fluid lining the epithelium covered six upper branches of respiratory tract (Q_M)	0·05–0·3 (ml)
Volume of the epithelium layer covered six upper branches of respiratory tract (Q_{LE})	0·05–0·3 (ml)
Volume of intercellular space in Q_{LE} compartment (Q_{LEI})	
in normal condition	0·003–0·02 (ml)
during inflammation	0·05–0·3 (ml)
Volume of fluid in airway lumen per macrophage	$5 \times 10^{-8}–3 \times 10^{-7}$ (ml)
Volume of intercellular space in Q_{LE} compartment per leukocyte	
in normal condition	$10^{-11}–10^{-9}$ (ml)
during inflammation	$3 \times 10^{-11}–2 \times 10^{-9}$ (ml)

- antibodies specific to IAV (F) (considered to be uniformly distributed between mucous, blood and LALT).

These make up the set of the state variables of the mathematical model of the antiviral immune response.

3. Generalized Picture of Uncomplicated Influenza A Virus Infection in Humans

In this section we suggest a quantitative definition of the processes of antiviral immune response during uncomplicated human IAV infection. There is a large variety of immunologic and virologic, experimental and clinical data characterizing the infection processes at different levels and from particular viewpoints and, consequently, partially and incompletely. But putting forward clear assumptions, it is possible to integrate particular *in vivo* and *in vitro* data sets including heterogeneous and incomplete observations into a theoretical model of the natural course of uncomplicated IAV infection in the state space of model variables. In other words, it is possible to derive a consistent homogeneous description, in quantitative terms, of the typical kinetics of an antiviral immune response during the infection. This generalized picture (GP) of uncomplicated IAV infection fixes our current quantitative understanding of the disease processes as a whole. The GP of an infectious disease may be considered as an intermediate level of data organization between the experimental facts and the mathematical model.

Definition

The generalized picture of a typical uncomplicated influenza A virus infection is a quantitative presentation, in the framework provided by the state variables of the mathematical model, of various virologic, immunologic and pathologic processes occurring after IAV invasion and resulting in an uncomplicated influenza infection.

First, let us define accurately, using the analysis of the previous section, the state space in which we define the nominal trajectory corresponding to uncomplicated IAV infection. It is ten-dimensional and has the following coordinates, the concentrations of the elements of our antiviral immune response model:

$V_f(t)$—infective IAV particles in the mucous compartment.

$M_V(t)$—stimulated (antigen presenting and IL-1 producing) macrophages in the LALT compartment.

$H_E(t)$—IAV-specific, activated (G_1-phase) helper T cells providing proliferation of cytotoxic T cells in the LALT compartment.

$H_B(t)$—IAV-specific, activated (G_1-phase) helper T cells providing proliferation and differentiation of B cells in the LALT compartment.

$E(t)$—activated (G_1-phase) CTL specific for IAV in the LALT comparment. The CTL population is considered to be functionally uniform. We assume that the concentration of mature CTL in the mucous compartment is directly related to that in LALT.

$B(t)$—IAV-specific B cells in the LALT compartment.

$P(t)$—plasma cells producing IAV-specific antibodies in the LALT compartment.

$F(t)$—antibodies to IAV, assumed to be the same for mucous, blood and LALT.

$C_V(t)$—IAV-infected epithelial cells of upper and central airways, producing the viruses.

$m(t)$—destroyed epithelial cells, characterizing the degree of damage of the airways.

3.1. KINETICS OF INFLUENZA A VIRUS REPLICATION

Data on IAV replication, in six adult volunteers, in relationship to the onset of clinical and IFN-responses, as well as nasal wash antibody responses, are given in Murphy & Webster (1985). The volunteers received 10^{10} virus part. (or 10^4 $TCID_{50}$) of wild-type A/Hong Kong/68-like virus intranasally on day 0. Virus replication peaked at about 48 hr after inoculation and declined thereafter, with little shedding after days 6 to 8. Peak virus titers range in symptomatic volunteers from 10^9 to 10^{13} virus part. (in log-average—10^{11}) of nasopharyngeal wash with a correlation observed between the level of virus shedding and the magnitude of clinical symptoms.

The experimental data of McLaren *et al.* (1978) on influenza virus replication in mouse are characterized by 10^8-fold increase of virus titers, with the peak at about 48 hr after infection, and decline to the inoculation level on the sixth day (see Fig. 1).

It is reported that influenza viruses could be detected as long as 10–14 days from the onset of infection and thereafter are completely eliminated (Luria *et al.*, 1978; McLaren *et al.*, 1978). These and some other data reported in Murphy & Webster (1985) may be generalized in the following way:

- the typical initial concentration of aerosol-delivered IAV is about 10^8 virus part ml^{-1};
- the second day after infection is the moment of the peak concentration of the viruses;

- the relative increase of IAV concentration is about 10^5;
- the IAV concentration drops considerably after the 6th day.

Three corresponding estimates for the kinetics of influenza A virus in airway secrets during uncomplicated influenza are given in Table 3.

3.2. KINETICS OF EPITHELIAL DAMAGE

The target cells for IAV are the epithelial cells of the upper airways and of the respiratory tract. The infected cells are destroyed by both the cytopathic effect of viruses and the result of immune (specific and nonspecific) reactions developing to suppress virus replication in sensitive tissue cells. The onset of illness is usually abrupt and is manifested by fever and other clinical signs. IAV induces pathologic changes throughout the respiratory tract. During bronchoscopy of persons with an uncomplicated influenza infection, acute diffuse inflammation of the larynx, trachea and bronchi, mucosal inflammation and edema, submucosal edema and hyperemia are observed (Murphy & Webster, 1985). The clinical

TABLE 3

Generalized picture of uncomplicated influenza A infection

Time (days)	Estimated value of variable	Comments
		Concentration of influenza A viruses in mucosa $\left(\frac{\text{particles}}{\text{ml}}\right)$
	V_f	
0	$0{\cdot}6 \times 10^8$	Infection dose
2	$0{\cdot}2 \times 10^{13}$	Peak of illness, period of maximum antigen concentration
6	$0{\cdot}6 \times 10^8$	Early stage of recovery, disappearance of viral particles
		Concentration of destroyed epithelial cells (Proportion of the steady-state concentration of epithelial cells)
	m	
1	0·1	Onset of specific disease symptoms
2	0·4	Peak of illness
5	0·1	Early recovery
		Concentration of antigen-presenting and IL-1 producing macrophages (Proportion of the steady-state concentration of lymph node macrophages)
	M_V	
0·5	10^{-2}	Onset of nonspecific disease symptoms
2	0·4	Peak of illness
		Concentration of activated, influenza A virus-specific Th1 cells in LALT (Relative to the steady-state concentration in lymph node)
	H_E	
0	0·1	The present estimates describe the initial activation of G_0-helper T cells
5	10	and proliferation of G_1-phase helper T cells
		Concentration of activated, influenza A virus-specific Th2 cells in LALT (Relative to the steady-state concentration in lymph node)
	H_B	
0	0·1	The present estimates describe the initial activation of G_0-helper T cells
5	10	and proliferation of G_1-phase helper T cells
		Concentration of activated, influenza A virus-specific CTLs in LALT (Relative to the steady-state concentration in lymph node)
	E	
0	0·1	The present estimates describe initial activation of G_0-phase CTLs
7	10	and proliferation of G_1-phase CTLs
		Concentration of activated, influenza A virus-specific B cells in LALT (Relative to the steady-state concentration in lymph node)
	B	
0	1	The present estimates describe
7	10^2	proliferation of B cells
		Concentration of plasma cells secreting influenza A virus-specific antibodies in LALT (Relative to the steady-state concentration in lymph node)
	P	
0	1	The present estimates describe
7	2×10^4	differentation of B cells

studies of disease severity and the degree of virus-induced hyperemia in the airways given by Marchuk & Berbentzova (1989) serve to support the following generalizations:

- the minimal clinical symptoms typical for the beginning of influenza result from the damage of about 10% of the epithelial cells;
- at the peak of the disease about 30%–50% of the epithelial of upper airways is destroyed;
- the resolution of disease may be characterized by as large as 10% damage of the normal epithelial cell population.

It was established, that desquamation of the epithelial cells takes place within the 1st day after the onset of clinical symptoms, while from days 3–5 remarkable cellular regeneration of the epithelium begins.

The strict correlation between the amount of virus shedding and the magnitude of clinical response allows one to relate the disease variable (m) values with those of the IAV kinetics (Table 3).

3.3. KINETICS OF MACROPHAGE ACTIVATION

An important aspect of developing the GP of uncomplicated IAV infection is coordination of the viral kinetics and macrophage activation. Direct data describing the dynamics of antigen-presenting macrophages (M_V) for influenza infection do not exist, as is the case for hepatitis B infection. Thus, two approaches for the estimation of their kinetics were used. The first approach was similar to one employed for creation of the generalized picture of acute hepatitis B, and the second was based on the pyrogenic effect of stimulated macrophages.

The most prominent sign of infection is a fever that often peaks within 24 hr to as high as 41°C, but more commonly is in the 38–40°C range (Murphy & Webster, 1985). It is known that for people weighing 70 kg there are about 3×10^9 macrophages in the lung. 10^6 stimulated macrophages per kg of body's weight may induce a 0·5–1°C rise in the temperature (Tinsley *et al.*, 1987). Using these data, it can be estimated that at the peak of influenza infection about 30–40% of the total lung's macrophage population is stimulated (Table 3).

3.4. KINETICS OF ANTIVIRAL IMMUNE RESPONSE

The limitation and the resolution of the infection process result from correlated responses of the non-specific and the immune defense systems. The non-specific response is related to interferon production, to intensive infiltration of the infection site by neutrophils and mononuclear cells, and to mucous surface hyperemia and inflammation. Normally, these result in the limitation of viral spread and the beginning of its elimination (Ada & Jones, 1986; Reynolds, 1989). However, the full clearance of the organism from viruses is provided by specific components of anti-IAV immune response.

We are interested in a quantitative description of the immune response during influenza A infection in an organism that is not primed to a given virus-subtype but one with a previous immunologic experience to other subtypes of IAV.

Conventionally, immunological memory to IAV in adults is accepted to exist both at T and B cell levels. However, Zinkernagel *et al.* (1985) suggest that antiviral T cell memory is more quantitative than qualitative, in that the precursor frequencies of relevant T cells are temporally increased for a short period of time after acute viral infection, and the kinetics of secondary antiviral T cellular responses compared with primary response are characterized by

(i) no appreciable acceleration,
(ii) no augmentation of the response.

For influenza-immune CTL it was shown that memory of previous influenza infection is reflected in increased numbers of progenitor cells that are available for clonal expansion. In humans a natural influenza infection induces T cell memory which may be characterized by about 10–10^2-fold increase of cross-reactive precursor frequency (specific to any viral determinant) with a half-life of CTL memory of about 0·5–3 years (Mitchell *et al.*, 1985; Ada & Jones, 1986; Murphy & Webster, 1985).

Analysis of experimental data on helper T cells dynamics in influenza shows that maximum activity of helper T cells is reached within 2–6 days after infection. The CTL activity peaks later, at 6–10 days (Ada & Jones, 1986). During these time intervals limited numbers of helper and cytotoxic T lymphocytes can be produced by proliferation of antigen-activated precursors. The kinetics of primary antiviral immune response to simple antigen in a lymph node was considered in detail in our previous paper on acute hepatitis B. It was characterized by a 10^4-fold increase of virus-specific T cells with respect to the homeostatic concentration.

Using points (i) and (ii) (above) of Zinkernagel *et al.* (1985), we suggest that in an organism with 10^2-fold increased population of IAV-specific T cell precursors, an infection with a new strain of IAV would normally induce an immune response in the

lymph nodes of LALT which is characterized by the following scale:

- 10^2-fold rise of helper T cells during the first 5 days,
- 10^2-fold rise of CTL during the first 7 days.

The corresponding data points are given in Table 3. They imply that the absolute magnitude of the T cell response over the first 7 days should be similar to that for acute hepatitis B, but the relative response is proportionally less compared to the increase in frequency of cross-reactive precursors.

The typical scale for increase in IAV-specific B cell precursor frequency after primary infection seems to be in 10–100 range (Ada & Jones, 1986). Taking into account the subtype-specificity of B cell memory, it seems reasonable to admit a 10-fold rise in the B cell population able to respond cross-reactively to a new strain of IAV due to previous antigenic experience. Then we suggest that the absolute pattern of B cell response should be similar to that developing in a lymph node stimulated by a simple viral antigen during acute HBV infection. Therefore, the B cell response in a lymph node of the LALT during influenza is assumed to be characterized by 10^3-fold increase with respect to steady-state concentration over the first 7 days. This estimate qualitatively corresponds to results of clinical investigation on humans (Murphy *et al.*, 1982) and experiments on mice (McLaren *et al.*, 1978). The latter showed that the anti-HA antibody concentration rose during an influenza infection by 10^2–10^3 times compared to the homeostatic value. This increase is caused by a clonal expansion process of anti-HA specific B- and plasma cells of similar scale, with the differences in basic compartment volumes and half-life times for plasma cells and antibodies taken into account. The corresponding estimates characterizing T cell and B cell accumulation processes during influenza are given in Table 3.

IAV replicates rapidly. Thus the duration of the activation process of helper T cells and of CTL precursors should be taken into account, because it is of the same scale as the time required for a 10–10^2-fold increase of viral population. The experimental data show that about 2–10% of lymph node lymphocytes are in the activated phase (G_1); the others are in G_0. We considered the steady-state populations of activated helper T cells and CTL to be 1/10 of the total, and this is reflected in Table 3.

Unfortunately, we are not able at the moment to suggest for the GP data set consistent data points on the time course of influenza-infected epithelial cells and antibodies to IAVs during an uncomplicated influenza A infection.

4. Analysis of Influenza A Virus Infection in Terms of the Model Parameters

4.1. MAIN SET OF EQUATIONS FOR ANTIVIRAL IMMUNE RESPONSE

A conceptual model of the basic immune processes operating during acute viral infection, with interactions described in terms of positive and negative influences, have been interpreted and organized into a population level mathematical model for the antiviral immune response (see Marchuk *et al.*, 1991*a*, for details). The interactions between the populations are described in the framework of the clonal selection theory, the birth–death balances of populations of cells and molecules, the additive character of interactions and their proportionality to population sizes, and an average fixed specificity for an antigen. The duration of cell division and differentiation is taken into account by delays. The set of equations of the mathematical model for specific components of the antiviral immune response, to be discussed in detail below, is as follows:

$$dV_f/dt = \nu C_V + nb_{CE}C_V E - \gamma_{VF}V_f F - \gamma_{VM}V_f - \gamma_{VC}V_f(C^* - C_V - m), \quad (1)$$

$$dC_V/dt = \sigma V_f(C^* - C_V - m) - b_{CE}C_V E - b_m C_V, \quad (2)$$

$$dm/dt = b_{CE}C_V E + b_m C_V - \alpha_m m,\ \xi(m) = 1 - m/C^*, \quad (3)$$

$$dM_V/dt = \gamma_{MV}M^* V_f - \alpha_M M_V, \quad (4)$$

$$dH_E/dt = b_H^E[\xi(m)\rho_H^E M_V(t-\tau_H^E)H_E(t-\tau_H^E) - M_V H_E] - b_p^{H_E}M_V H_E E + \alpha_H^E(H_E^* - H_E), \quad (5)$$

$$dH_B/dt = b_H^B[\xi(m)\rho_H^B M_V(t-\tau_H^B)H_B(t-\tau_H^B) - M_V H_B] - b_p^{H_B}M_V H_B B + \alpha_H^B(H_B^* - H_B), \quad (6)$$

$$dE/dt = b_p^E[\xi(m)\rho_E M_V(t-\tau_E)H_E(t-\tau_E) \times E(t-\tau_E) - M_V H_E E] - b_{EC}C_V E + \alpha_E(E^* - E), \quad (7)$$

$$dB/dt = b_p^B[\xi(m)\rho_B M_V(t-\tau_B)H_B(t-\tau_B) \times B(t-\tau_B) - M_V H_B B] + \alpha_B(B^* - B), \quad (8)$$

$$dP/dt = b_p^P\xi(m)\rho_P M_V(t-\tau_P)H_B(t-\tau_P) \times B(t-\tau_P) + \alpha_P(P^* - P), \quad (9)$$

$$dF/dt = \rho_F P - \gamma_{FV}FV_f - \alpha_F F. \quad (10)$$

Our approach to parametric analysis of the model is based on taking into account the localization of immune response and disease variables.

4.2. VIRUS-SENSITIVE TISSUE INTERACTIONS

First, consideration will be given to the parameters characterizing virus-sensitive tissue processes in the mathematical model of antiviral immune response for influenza A virus infection. In a previous paper (Marchuk *et al.*, 1991*a*) a similar analysis was done for acute hepatitis B virus infection. Tissue cell tropism, replication time, kinetics of expression of viral antigens on target cells, and the extent of infected cell destruction caused by the virus differ considerably for IAV and HBV and determine both the nature of antiviral immunity and the disease process.

Equation (1) for *V_f—free influenza A viruses concentration in the respiratory mucosa.* It is established that epithelial cells express viral antigens 4 hr after an infection with IAV. Intensive replication and secretion of viruses take place 6–12 hr after infection. During a day about 10^3–10^4 influenza viruses are synthesized by a single infected cell (Zdanov & Bukrinskaja, 1969). Using this information we choose the secretion rate constant v in eqn (1) for influenza A viruses to be about 10^2–10^4 viruses $\cdot$ cell^{-1} $\cdot$ day^{-1}.

The final assembling step of the influenza A virion takes place on the membrane of an infected epithelial cell while being released from it. This is a general mechanism for ortomyxoviruses (Kingsbury, 1986). Therefore, there should be no complete virions inside the infected cell, and the lethal damage of such a cell by CTL shouldn't lead to any release of infective IAV from the cell. Consequently, we take the value of the corresponding model parameter n in eqn (1) to be 0.

The rate constant of IAV neutralization by specific antibodies can be estimated by the same scheme that was employed for HBV. It is known that for neutralization of a single IAV binding with 1–10 IgG molecules is generally sufficient (Wohlfart, 1988). Taking the association rate constant for high affinity antibodies to be $\gamma_{FV} \approx 8{\cdot}6 \times 10^{10}$–$8{\cdot}6 \times 10^{12}$ M^{-1} day^{-1} under the hypothesis of irreversibility of binding, one can obtain the range for γ_{VF} in eqn (1) to be $8{\cdot}6 \times 10^9$–$8{\cdot}6 \times 10^{12}$ M^{-1} day^{-1}.

Physical defense constitutes an important mechanism for neutralizing or removing injurious agents from the respiratory tract (Newhouse *et al.*, 1976; Clarke, 1983; Reynolds, 1989; Toews, 1989). It includes the mucociliary transport system, supplemented by the cough mechanism. For influenza infection the mucociliary clearance of free viral particles may be considered as the major nonspecific method of infective virion removal. Reports of Newhouse *et al.* (1976) and Clarke (1983) indicate that particles deposited in the trachea and initial bronchial divisions are cleared with a half-time of 30 min, whereas the clearance of the airways down to about the 16th division takes place over 24 hr. Uncomplicated IAV infection involves six bronchial divisions so that we chose the typical time of physical clearance to be about 4–24 hr. Then, the parameter γ_{VM} corresponding to nonspecific clearance rate of viruses ranges between 1–6 day^{-1}.

The parameter γ_{VC} in eqn (1) characterizes the IAV adsorption rate by normal epithelial cells. It is known that in *in vitro* experiments a single epithelial cell can adsorb from 1–10 influenza virions. Multiple infection leads to the production of a large number of defective viral particles. The typical time of IAV virus-epithelial cell interaction is about 10 min (Zdanov & Bukrinskaja, 1969). On the other hand, an epithelial cell becomes infected, i.e. the replication of virus and the virus antigen expression take place 4–6 hr following the penetration of bound virus. To balance the number of cells that become infected and the number of viruses that were absorbed we related the corresponding parameters σ and γ_{VC} in the following way: $\gamma_{VC} = k \times \sigma$, where $1 < k < 10$.

Equation (2) for *C_V—virus infected epithelial cells.* A typical uncomplicated IAV infection is considered to be an infection involving epithelial cells in the space from the trachea up to the sixth division of the bronchial tree, with the average concentration of the cells being about 10^9–10^{10} cell $\cdot$ ml^{-1}. The infection process for epithelial cells is characterized by the rate constant σ in eqn (2). The cell begins to synthesize IAV 6 hr following the penetration of the virion, and this value may be considered to be the time scale, $t_{C \to C_V}$, of the single cell infection process. We are interested in a quantitative description of the infection of about 30–50% of sensitive cells C^* in the lung epithelium compartment: $[\Delta C \approx (0{\cdot}3\text{–}0{\cdot}5) \times C^*]$, which is typical for uncomplicated influenza, during the time interval of $\Delta t \approx t_{C \to C_V}$. To derive corresponding estimate for σ we employed the scheme

$$\sigma = \frac{1}{t_{C \to C_V} \times \Delta C}$$

suggested by Marchuk *et al.* (1991*a*). Under the assumption of one virus to one epithelial cell we obtained the estimate: $\sigma \approx 5 \times 10^6$–$10^7$ M^{-1} day^{-1}.

Influenza A virus is highly cytopathic. According to Zdanov & Bukrinskaja (1969) the average life time of an infected epithelial cell is about 1 day. Thus the

initial guess for the infected cell destruction rate b_m in eqn (2) may be taken as $b_m \approx 1$ day^{-1}.

The duration of a single division of an epithelial cell during the recovery phase of the disease is about 0·3–1 day (Kilburne, 1987; Keenan *et al.*, 1982*a*, *b*; Lechner *et al.*, 1982). The corresponding parameter α_m in eqn (3), characterizing the regeneration rate of the epithelium, was thus taken to be about 1–3 day^{-1}.

To estimate the parameter b_{CE} in eqns (1), (2), characterizing the CTL-mediated destruction of infected epithelial cells by delivery of lethal hits on a cell-to-cell basis (without taking inflammation into account) we employed the scheme

$$b_{CE} = \frac{1}{(t_{E:Q_{LN}\to Q_{LE}} + t_{E:C_V\to m}) \times E^{\text{suf}}}.$$

Here $t_{E:Q_{LN}\to Q_{LE}}$ is the typical transfer time of CTL from the LALT compartment to the mucous compartment, about 2–12 hr (Rusznyak *et al.*, 1957), $t_{E:C_V\to m}$—is the duration of the lethal hit process ($\approx$20–30 min according to Martz *et al.* (1983), and E^{suf} is the estimate of the number of CTLs sufficient to destroy all infected epithelial cells. This was considered to be about 0·1 × (0·3–0·5)C^*, with the ability of a single CTL to deliver several ($\sim$10) lethal hits taken into account. Thus

$$b_{CE} \approx 2 \times 10^7\text{–}4 \times 10^8\ \text{M}^{-1}\,\text{day}^{-1}.$$

Destruction of infected epithelial cells during influenza appear to be realized by the coordinated action of specific as well as nonspecific mechanisms, and both seem to be equally important. CTLs are considered to be essential in recovery from influenza infection: in human volunteers CTL memory correlated with rapid clearing of administered virus in individuals with no antibody immunity (Mitchell *et al.*, 1985). CTLs are able to kill virally infected cells and destroy tissue by direct cytotoxicity and recruitment of inflammatory cells to prevent further virus replication. Doherty (1985) reports that CTLs promote inflammation in experimental influenza infection. Both virus induced inflammatory process and virus clearance are considered to be functions of the class I MHC-restricted T cell population. The desquamation of the epithelial cells is the direct result of the CTL-induced nonspecific destruction of epithelial cells in the infected area of tissue. An uncomplicated influenza infection is characterized by acute diffuse inflammation of larynx, trachea and bronchi as well as mucosal inflammation and edema. On the other hand, one can compare an estimate of infected epithelial cells which should be destroyed, about 10^{10} cells, and an estimate of the CTL progeny able to kill them generated in the course of the immune response during first 5–7 days, which is about 10^8. Then the conclusion can be drawn that a single CTL should kill about 100 infected epithelial cells. It seems unlikely that its potential is sufficient to do this (Martz *et al.*, 1983; Perelson & Bell, 1982). Clearly, to destroy such an abundance of infected cells, CTLs, together with direct lethal damage of infected cells by contact interaction, should induce nonspecific processes of infected epithelial cell destruction. Inflammation may be considered as the basic mechanism of the destruction intensification process. Another mechanism is the secretion of IFN-γ by CTL which increases target cell expression of MHC antigens, possibly making these cells more sensitive to CTL, and activates NK cells (Mitchell *et al.*, 1985). To take into consideration the intensification effect of inflammation on both the rate of CTL-controlled destruction of infected epithelial cells and the antibody-mediated neutralization of free viruses, the corresponding terms in eqns (2), (3) and (1) for C_V, m and V_f were modified in the following way (according to Marchuk & Petrov, 1983):

$$b_{CE}CVE \to f_C(l)b_{CE}C_VE,$$

$$\gamma_{VF}FV \to f_V(l)\gamma_{VF}FV \text{ with } l = C_V/C^*.$$

The functions $f_C(l) \equiv (1 + \mu_C(C_V/C^*))$, $f_V(l) \equiv (1 + \mu_V(C_V/C^*))$ phenomenologically link the processes of inflammation and tissue destruction to the degree of sensitive tissue infection C_V. As an initial guess for μ_C and μ_V we suggest an estimate of the ratio of peak number of infected cell to the maximum number of CTLs over the first 5 days after the beginning of IAV infection. This ratio is about 10^2.

Now we consider the parameters governing the realization of virus specific cellular and humoral immune responses during IAV infection in the framework of the antiviral immune response model [eqns (4–10)].

The estimates for all these were constructed in previous papers (Marchuk *et al.*, 1991*a*, *b*) for the acute hepatitis B infection. Influenza A virus has a different antigenic structure and provides a different time scale as compared to HBV. We postulated that:

(i) The particular antigenicity selects the frequency of responders and thus defines the homeostatic size of T and B cells specific for IAV.
(ii) Influenza A is a fast infection, i.e. the incubation period is short and virus replicates rapidly, so the estimates of parameters should be modified for those that were constructed with the slow character of hepatitis B virus in mind. To this group belong the parameters characterizing the

progeny size and duration of progeny formation for CTLs and B cells.

(iii) The antigen-induced activation of macrophages and the proliferation and differentiation of T and B cells in LNs are not related directly to the specificity of pathological processes induced by particular viruses. The admissible ranges of stimulation rate constants characterizing the interactions in lymphoid tissue are considered to be invariant for different lymph nodes and antigen specificities during the inductive phase of the immune response. This point may be questioned, because variations in replication times of immunocompetent cells are allowed as an adaptation mechanism providing adequate defense against highly cytopathic viruses (Zinkernagel *et al.*, 1985). However supporting quantitative data are not known to us.

4.3. IMMUNE HOMEOSTASIS

It is established that natural influenza boosts T cell and B cell memory (Ada & Jones, 1986). A memory of a previous infection implies that increased numbers of progenitor cells are available for clonal expansion. The data reported elsewhere show considerable variation in the magnitude of memory T- and B cells levels over time, but generally, the relative increase of precursor frequency is 2–100-fold. The majority of IAV-induced CTLs are fully cross-reactive and would provide heterotypic immunity, in contrast to antibodies (and consequently B memory cells) which are protective against reinfection by strains closely related to the stimulating IAV. The specificity of IAV-induced helper T cells parallels that reported for CTL. The existence of specific activity of helper T cells taken in immunized mice at 2 years may also be interpreted as memory of a helper cell subset (Ada & Jones, 1986). The half-life of influenza-induced human CTL memory is reported to be about 0·5–3 years. The existence of memory T- and B cells in adult humans with different patterns of specificity should be taken into account when constructing estimates of homeostatic levels of lymphocytes in the LALT, which specifically respond by clonal expansion during uncomplicated IAV infection.

The concentration of macrophages able to present foreign antigens in LALT [M^* in eqn (3)] was considered to be the same as in other LNs. According to Sapin *et al.* (1978), and Shevach (1984), the following estimate can be used:

$$M^* \approx 5 \times 10^{-16}\text{–}3 \times 10^{-15}\,\text{M}.$$

The numbers of helper T cells (Th1 and Th2) and CTL-precursors in a lymph node able to respond to simple antigen were discussed by Marchuk *et al.* (1991*a*). Taking into account memory and cross-reactivity phenomena in the case of influenza A in adults, we suggest that the numbers of H_E^*, H_B^* and E^* should be increased by 100-fold. Thus, the following estimates of homeostatic sizes of T cell subsets specific for IAV [eqns (5), (6), (7)] were used: $H_E^* \approx 10^{-16}\text{–}10^{-15}\,\text{M}$, $H_B^* \approx 10^{-17}\text{–}10^{-16}\,\text{M}$, $E^* \approx 10^{-16}\text{–}10^{-15}\,\text{M}$.

The effect of the memory of a previous influenza infection on the homeostatic size of B cell and antibody populations able to recognize a new subtype of influenza A virus—B^*, F^* in eqns (8), (10)—should be manifested to a lesser extent than for T cells due to poor cross-reactivity. This point may be accounted for by a 10-fold rise in the frequency of B cells and antibodies specific for an IAV subtype, compared to that in the case of simple antigens for organism that is not primed: $B^* \approx 5 \times 10^{-18}\text{–}5 \times 10^{-17}\,\text{M}$, $F^* \approx 10^8\text{–}10^9{}_{\text{molecules}}\,\text{ml}^{-1} \approx 1{\cdot}7 \times 10^{-13}\text{–}1{\cdot}7 \times 10^{-12}\,\text{M}$.

An estimate of the homeostatic concentration of plasma cells (P^*) in eqn (9), providing the given (F^*) level in blood, mucous and LALT of antibodies specific for IAV, can be obtained using the secretion rate ρ_F and the volumes of the corresponding compartments ($Q_{\text{comp.}}$ in Tables 2, 5):

$$P^* = \frac{\alpha_F(Q_{\text{blood}} + Q_M + Q_{LALT})}{\rho_F Q_{LALT}} \approx 2\text{–}43\ \text{cell ml}^{-1} \approx 3 \times 10^{-21}\text{–}7 \times 10^{-20}\,\text{M}.$$

Estimates of decay rates for helper T cells [α_H^E, α_H^B in eqns (5), (6)], CTL [α_E in eqn (7)], B cells [α_B in eqn (8)], plasma cells [α_P in eqn (9)], antibodies [α_F in eqn (10)] and antigen-presenting macrophages in eqn (4) were taken to be the same as in the case of hepatitis B immunity, due to the identity of their biological meaning.

4.4. ANTIGEN-DRIVEN CLONAL EXPANSION

Generation of the immune response in IAV infection includes the steps of initial clonal activation, proliferation and differentiation of various lymphocyte subsets. Data from animal studies shows that helper T cell activity during influenza is characterized by peak activity titers at day 2, while CTL activity develops early after the onset of influenza infection and reaches a peak between days 4 and 10, generally before specific antibodies are detectable (Ada & Jones, 1986). The initial activation of helper T cells during hepatitis B infection was considered as instantaneous in comparison to the low replication rate of the virus. The initial activation of T cells depends on co-recognition of foreign antigen with MHC

molecules on the surface of macrophages and usually takes 4–24 hr (Depper *et al.*, 1984; Shevach, 1984) to progress from the G_0 to G_1 phase of cell cycle. This time is comparable with the time for a 10–10^3-fold increase of IAV antigen concentration due to fast replication rate of the virus. Thus, a sharper time scale is provided by IAV as compared to HBV for the timing of immune response generation. Activated T cells produce different factors which are extremely important for the kinetics of the influenza A infection: helper T cells secrete IL-2 and other lymphokines and CTL produce IFN-γ, which increases the expression of MHC antigens acting to enhance virus-infected cells destruction (Mitchell *et al.*, 1985). The initial immune activation has an important implication for the IAV infection course (Murphy & Webster, 1985). The kinetics of initial activation of helper T cells and CTLs was described by specific initial functions for delay terms in equations (5)–(7):

$$\varphi^E_H(t) = M_V(t)H_E(t),\ -\tau^E_H \leqslant t \leqslant 0,$$

$$\varphi^B_H(t) = M_V(t)H_B(t),\ -\tau^B_H \leqslant t \leqslant 0,$$

$$\varphi_E(t) = M_V(t)H_E(t)E(t),\ -\tau_E \leqslant t \leqslant 0.$$

Typically, about 90% of T cells in a LN are in G_0 phase, while the other 10% are activated, i.e. in G_1 phase (Hofman *et al.*, 1985). This cell cycle distribution of T cells leads to the delayed and monotone character of appearance of completely activated T cells over the 1st day after the onset of infection, which is schematically represented in Fig. 3. The bell-shaped initial functions of the following type (Richtmayer, 1978; Vladimirov, 1988) were taken:

$$\begin{cases} \dfrac{1}{C}\exp^{\frac{1}{1-t^2}}, & \text{for } 0 < |t| < 1, \\ 0, & \text{for } |t| \geqslant 1. \end{cases}$$

They have been specified to meet the requirements which are similar for H_E, H_B and E, so only the case of H_E (Th1 cells) is explained: $\varphi^E_H(t)$ being inserted in corresponding eqn (5) and integrated over the time interval 0–τ^E_H should add $0{\cdot}9 \times H^*_E$ cells to the population of the cells being activated at the moment of infection. Therefore, the initial function φ^E_H, taken to satisfy the equality

$$\int_0^{\tau^E_H} b^E_H \rho^E_H \varphi^E_H(t - \tau^E_H)\mathrm{d}t = 0{\cdot}9 \times H^*_E,$$

can be specified as follows:

$$\varphi^E_H(t) = \begin{cases} \dfrac{2{\cdot}52 \times 0{\cdot}9 \times H^*_E}{0{\cdot}33 \times \tau^E_H \times b^E_H \times \rho^E_H} \times \exp^{\frac{-1}{1-[(t-\tau^E_H/3)/(2/3\tau^E_H)]^2}}, & \text{for } -2/3\tau^E_H < t < 1, \\ 0, & \text{for } t \leqslant -2/3\tau^E_H,\ t \geqslant 0. \end{cases}$$

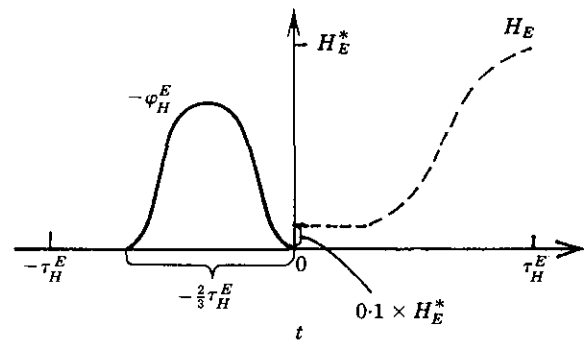

FIG. 3. The scheme (using the example of H_E cells) for the kinetics of initial activation (– – –) of T cells being distributed at the moment of infection over resting and activated states. The effect of the distribution on the kinetics of antigen-driven activation is modeled by initial functions for the delay terms represented by (—).

The initial concentrations of $H_E(0)$, $H_B(0)$ and $E(0)$ corresponding to the number of non-specifically activated T cells in lymph node at the moment of infection were taken to be 0·1 of their corresponding homeostatic sizes (H^*_E, H^*_B, E^*) estimated above.

The initial distribution of B cells seems to be not so important to the dynamics of the infection because they do not participate in the initial regulation of the immune response, and the humoral immune response usually appears to be a more slow process than T cell immunity.

The fast character of IAV growth makes it necessary to adjust the interpretation of the proliferation and differentiation of T- and B cells in the model from a clone formation level to a single division level. It means that, instead of considering the parameters ρ^E_H, τ^E_H, ρ^B_H, τ^B_H, ρ_E, τ_E, ρ_B, τ_B, ρ_P, τ_P as the numbers of daughter cells in clone and the durations of clone formation (in the case of hepatitis B), we should rather treat them as parameters of a single division and thus, refine the time resolution by considering elementary steps of clone formation processes. According to Shevach (1984), the duration of single division of activated helper T cell, τ_H, ranges from 10–20 hr. This uncertainty, being not large for hepatitis B immune response, seems to be wide in the case of IAV infection. To allow for this uncertainty we suggested in eqns (5) and (6) that from one to two consecutive divisions may take place during the τ^E_H, τ^B_H, and therefore the number of daughter cells ρ^E_H, ρ^B_H may be 2 or 4.

The same arguments could be used while analyzing the parameters τ_E and ρ_E in eqn (7) for CTL. The duration of a single division for CTL, τ_E, is 12–24 hr, and ρ_E is 2–4.

A stimulated B cell undergoes several divisions forming a clone of daughter B cells, plasma cells and memory cells. The part of clone differentiating into plasma cells is about 10% (Sengbusch, 1979). However, to account for the fact that in adults the immune response to IAV, in helper T cell and B cell subsets, has the features of a secondary immune response, we supposed that this portion may be increased to 30–40%. The duration of a single division of a B cell is about $\tau_B \approx 12$–24 hr (Mosier, 1986). Thus, to describe the proliferation of B cells and the appearance of plasma cells in eqns (8), (9) we took the estimates:

$$\rho_B = 1{\cdot}5\text{–}3,\ \rho_P = 0{\cdot}5 - 1,\ \tau_B = \tau_P = 0{\cdot}5\text{–}1\ \text{day}^{-1}.$$

The admissible range for the immune response stimulation rate parameters b_H^E, b_H^B, b_p^E, b_p^B, b_p^P may be constructed using the same approach that was employed for hepatitis B (Marchuk *et al.*, 1991*a*). Those estimates were derived without any definite relation to any particular antigenic specificity of the virus, and may be used as initial guess for influenza infection modeling. In Zinkernagel *et al.* (1985) it was pointed out that for acute infectious agents, one does not have to evoke sophisticated suppressor cells or cellular network circuits to regulate an immune response after fast elimination of acute cytopathic viruses. According to the *Generalized Picture*, IAVs are presented in concentrations exceeding the stimulation threshold for over 6 days, whereas 5–7 days are required for mounting an immune response. Therefore, the values of the suppression parameters $b_p^{H_E}$, $b_p^{H_B}$ in eqns (5) and (6), were taken to be effectively "zero", and equal to each other (compared to the case of HBV infection, for which the prolonged presence of antigen during the recovery phase is observed and suppression loops need to be involved).

The parameters of the model, their ranges and the initial values taken for simulations of the specific components of antiviral immune response during uncomplicated IAV infection are listed in Table 4.

4.5. PARAMETERS VALUES FITTED TO UNCOMPLICATED INFLUENZA A VIRUS INFECTION DATA

Initial estimates of the model parameters derived in the Sections 4.2–4.4 were refined according to the kinetic pattern of uncomplicated IAV infection represented by the generalized picture data (Table 3). The data are few in number, so the parameter candidates to be varied during the fitting must be carefully selected according to relations between the viral, immunologic and clinical processes and the underlying model parameters being considered to monitor the kinetics of the processes. By trial-and-error sequential fitting of the model to GP data, using the procedures described in the Appendix, a number of parameter values sets can be obtained. One of them is given in Romanyukha *et al.* (1992) and although closely fits the data, is characterized by biologically unrealistic values of some parameters. Prior knowledge about the antiviral immune response parameters for acute hepatitis B virus infection was used to improve the correctness of the estimates. We tried to obtain a consistent set of parameters values that gives a reasonable behavior with respect to the GP kinetics, while the differences in the antigen-driven lymphocyte stimulation rates in lymph nodes, as compared to HBV infection parameters, are minimal. The final list of parameter values adjusted to the GP data is given in Table 5. The corresponding solution with the GP data, is shown in Fig. 4. There are minor changes, less than 50%, in the values of b_m, α_m, γ_{VM}, as compared to their initial estimates. The refined values of the parameters for the IAV replication rate, (ν), the infection rate, (σ), differ considerably from their initial estimates—by 10 and 10^3-fold, respectively. The latter differences mean that the scheme employed for the initial estimation of σ is rather crude and should consider factors such as spatial structure, pathways of virus propagation (direct cell-to-cell), component transfer, etc, for the infection rate to be assessed more adequately. As large as an 800-fold increase in the value of the plasma cell generation rate (b_p^P) was necessary to fit the GP data. The final value of b_p^P is equal to b_p^B, which seems, however, to be more realistic than the about 800-fold difference of b_p^P and b_p^B in the case of the acute hepatitis B parameters set. Most disturbing is the very crude estimate of virus-infected epithelial cell killing rate mediated by CTL, b_{CE}. This fact illustrates that the kinetics of cell-mediated destruction process is not adequately represented by the scheme implemented for assessing the parameter estimate. Indeed, non-specific processes, like epithelial desquamation, local cytotoxic $T_{y\sigma}$ low-specificity reactions, as well as details of the spatial structure of the tissue, CTL recruitment, etc, should be accounted more precisely.

We consider the achieved degree of fitness as being good. Next, it would be necessary to validate the model by testing its predictive ability against experimental data which were not used directly for identification of parameters, and its behavior for clearly established infection phenomena (e.g. dose-incubation period relationship, protection by immune memory, etc).

TABLE 4

Constructed initial estimates of model parameters for simulation of the immune response in influenza A infection

	Physical meaning of parameters	Permissible values range	Initial value (unit)
M^*	concentration of class I or class II bearing macrophages (in LN)	5×10^{-16}–3×10^{-15}	10^{-15} (M)
H_E^*	concentration of influenza A virus (IAV) specific Th1 helper cells cooperating with cytotoxic T cells (in LN)	10^{-16}–10^{-15}	10^{-16} (M)
H_B^*	concentration of IAV specific Th2 helper cells cooperating with B cells (in LN)	10^{-17}–10^{-16}	10^{-17} (M)
E^*	concentration of IAV specific cytotoxic T cells (precursors) (in LN)	10^{-16}–10^{-15}	10^{-16} (M)
B^*	concentration of IAV specific B cells (in LN)	$0{\cdot}5 \times 10^{-17}$–$0{\cdot}5 \times 10^{-16}$	10^{-17} (M)
P^*	concentration of IAV specific plasma cells (convent.)	3×10^{-21}–7×10^{-20}	$1{\cdot}8 \times 10^{-20}$ (M)
F^*	concentration of IAV specific antibodies (in any compartment)	$1{\cdot}7 \times 10^{-13}$–$1{\cdot}7 \times 10^{-12}$	$8{\cdot}5 \times 10^{-13}$ (M)
C^*	concentration of epithelial cells	$1{\cdot}7 \times 10^{-12}$–$1{\cdot}7 \times 10^{-11}$	$1{\cdot}7 \times 10^{-11}$ (M)
α_M	rate constant of stimulated state loss for macrophages	1·0–1·5	1 (day^{-1})
α_H^E	rate constant of activated state loss for Th1 cells	0·8–1·2	1 (day^{-1})
α_H^B	rate constant of activated state loss for Th2 cells	0·8–1·2	1 (day^{-1})
α_E	rate constant of natural death for cytotoxic T cells	0·33–0·5	0·4 (day^{-1})
α_B	rate constant of natural death for B cells	0·05–0·1	0·1 (day^{-1})
α_P	rate constant of natural death for plasma cells	0·33–0·5	0·4 (day^{-1})
α_F	rate constant of natural death for antibodies	0·043	0·043 (day^{-1})
τ_H^E	duration of Th1 cell division(s)	0·4–0·8	0·6 (day)
τ_H^B	duration of Th2 cell division(s)	0·4–0·8	0·6 (day)
τ_E	duration of CTL division(s)	0·5–1	0·5 (day)
τ_B	duration of B cell division(s)	0·5–1	0·5 (day)
τ_P	duration of B cell division(s) and differentiation resulting in plasma cells appearance	0·5–1	0·5 (day)
ρ_H^E	number of Th1 cells created by division(s series)	2–4	4
ρ_H^B	number of Th2 cells created by division(s series)	2–4	4
ρ_E	number of CTLs created by division(s series)	2–4	2
ρ_B	proportion of B cells in clone created by series of 1 or 2 divisions	1·5–3	3
ρ_P	proportion of plasma cells in clone created by series of 1 or 2 divisions	0·5–1	1
ρ_F	rate of IgG production per plasma cell	$0{\cdot}85 \times 10^8$–$1{\cdot}7 \times 10^8$	$1{\cdot}7 \times 10^8$ (molecules/cell*day)
b_H^E	rate constant of Th1 cells stimulation	4×10^{14}–3×10^{15}	10^{15} ($M^{-1}\,day^{-1}$)
b_H^B	rate constant of Th2 cells stimulation	4×10^{14}–3×10^{15}	10^{15} ($M^{-1}\,day^{-1}$)
b_P^E	rate constant of CTL stimulation	5×10^{31}–7×10^{33}	10^{32} ($M^{-2}\,day^{-1}$)
b_P^B	rate constant of B cells stimulation	5×10^{31}–10^{33}	10^{32} ($M^{-2}\,day^{-1}$)
b_P^P	rate constant of B cells stimulation resulting in B cell proliferation and differentiation into plasma cells	5×10^{31}–10^{33}	10^{32} ($M^{-2}\,day^{-1}$)
$b_P^{H_E}$	parameter characterizing the suppression effect on Th1 cells		10^{25} ($M^{-2}\,day^{-1}$)
$b_P^{H_B}$	parameter characterizing the suppression effect on Th2 cells		10^{25} ($M^{-2}\,day^{-1}$)
γ_{MV}	rate constant of macrophage stimulation	10^8–4×10^{13}	10^{10} ($M^{-1}\,day^{-1}$)
γ_{FV}	rate constant of IgG binding to IAV	$8{\cdot}6 \times 10^{10}$–$8{\cdot}6 \times 10^{12}$	$8{\cdot}6 \times 10^{11}$ ($M^{-1}\,day^{-1}$)
σ	rate constant of epithelial cells infection with IAV	5×10^6–10^7	10^7 ($M^{-1}\,day^{-1}$)
b_{CE}	rate constant of infected epithelial cells damage by CTL	2×10^7–4×10^8	10^8 ($M^{-1}\,day^{-1}$)
b_{EC}	rate constant of CTL death due to lytic interactions with infected epithelial cells	2×10^6–4×10^8	10^8 ($M^{-1}\,day^{-1}$)
b_m	rate constant of infected epithelial cell damage due to IAV cytopathicity	0·5–2	1 (day^{-1})
α_m	rate constant of epithelial cell regeneration	1–3	3 (day^{-1})
ν	rate constant of IAV particles secretion per infected epithelial cell	10^2–10^4	6×10^3 (day^{-1})
n	number of IAV particles released from infected epithelial cells damaged by CTL	0	0
γ_{VC}	rate constant of IAV adsorption by epithelial cell	5×10^7–10^8	8×10^7 ($M^{-1}\,day^{-1}$)
γ_{VM}	rate constant of nonspecific IAV removal	2–4	2 (day^{-1})
γ_{VF}	rate constant of IAV neutralisation by anti-IAV IgG	$8{\cdot}6 \times 10^9$–$8{\cdot}6 \times 10^{12}$	$8{\cdot}6 \times 10^{11}$ ($M^{-1}\,day^{-1}$)
μ_V	amplification parameter for free viruses neutralization	10^2	10^2
μ_C	amplification parameter for infected cells destruction	10^2	10^2
γ_{M_I}	rate constant of IFN producing state induction in macrophages	$1{\cdot}4 \times 10^{11}$–$1{\cdot}4 \times 10^{13}$	2×10^{11} ($M^{-1}\,day^{-1}$)
α_{M_I}	rate constant of IFN producing state loss for macrophages	0·3–0·5	0·5 (day^{-1})
ρ_I	rate of IFN production per macrophage	7×10^{-6}–3×10^{-4}	8×10^{-5} IU/(cell*day)
α_I	rate constant of natural decay of IFN	100–10	24 (day^{-1})
σ_I	rate constant of IFN binding with epithelial cells	10^{10}–10^{12}	10^{12} ($M^{-1}\,day^{-1}$)
σ_R	rate constant of virus resistant state induction in epithelial cells		2×10^{10} ($M^{-1}\,day^{-1}$)
α_R	rate constant of epithelial cells virus resistant state decay		1 (day^{-1})

An analysis of the model solution (Fig. 4) allows one to conclude that the propagation of infection in virus-sensitive tissue is terminated in the first five days in the model by a limited number of susceptible cells C^* (before the specific immunity is brought into play). Working out of maximal eigenvalues

TABLE 5

Model parameters values for simulating an uncomplicated influenza A infection

Parameter	Estimate	Parameter	Estimate	[Init. estimate]
M^*	10^{-15} M	ρ_E, ρ_B	2,3	
H_E^*	10^{-16} M	ρ_P	1	
H_B^*	10^{-17} M	ρ_F	$1{\cdot}7 \times 10^8$ molecule × cell^{-1} × day^{-1}	
E^*	10^{-16} M	b_H^E	$2{\cdot}7 \times 10^{16}$ M^{-1} day^{-1}	
B^*	10^{-17} M	b_H^B	$2{\cdot}7 \times 10^{16}$ M^{-1} day^{-1}	
P^*	$1{\cdot}8139 \times 10^{-20}$ M	b_p^E	$5{\cdot}0 \times 10^{33}$ M^{-2} day^{-1}	
F^*	$8{\cdot}5 \times 10^{-13}$ M	b_p^B	$8{\cdot}0 \times 10^{32}$ M^{-2} day^{-1}	
C^*	$1{\cdot}7 \times 10^{-11}$	b_p^P	$8{\cdot}0 \times 10^{32}$ M^{-2} day^{-1}	[10^{30}]
α_M	3·3 day^{-1} [1]	γ_{MV}	$3{\cdot}4 \times 10^8$ M^{-1} day^{-1}	[10^{10}]
α_H^E	1·0 day^{-1}	γ_{FV}	$8{\cdot}6 \times 10^{11}$ M^{-1} day^{-1}	
α_H^B	1·0 day^{-1}	σ	$2{\cdot}0 \times 10^{10}$ M^{-1} day^{-1}	[10^7]
α_E	0·4 day^{-1}	b_{CE}	$6{\cdot}6 \times 10^{14}$ M^{-1} day^{-1}	[10^8]
α_B	0·1 day^{-1}	b_m	1·5 day^{-1}	[1·0]
α_P	0·4 day^{-1}	α_m	4·0 day^{-1}	[3·0]
α_F	0·043 day^{-1}	ν	510 day^{-1}	[$6{\cdot}0 \times 10^3$]
τ_H^E	0·6 day	γ_{VC}	$6{\cdot}0 \times 10^{10}$ M^{-1} day^{-1}	[$8{\cdot}0 \times 10^7$]
τ_H^B	0·6 day	γ_{VM}	1·7 day^{-1}	[2·0]
τ_E	0·5 day	γ_{VF}	$8{\cdot}6 \times 10^{11}$ M^{-1} day^{-1}	
τ_B	0·5 day	$b_p^{H_E}$	10^{25} M^{-2} day^{-1}	
τ_P	0·5 day	$b_p^{H_B}$	10^{25} M^{-2} day^{-1}	
ρ_H^E	4 [2]	ρ_H^B	4	[2]
μ_V	$1{\cdot}0 \times 10^2$	b_{EC}	$1{\cdot}6 \times 10^{11}$ M^{-1} day^{-1}	
μ_C	$1{\cdot}0 \times 10^2$	n	0	
V_I^0	$1{\cdot}0 \times 10^{-13}$ M			
M_I^*	$1{\cdot}7 \times 10^{-12}$ M			
γ_{MI}	$2{\cdot}0 \times 10^{11}$ M^{-1} day^{-1}	α_{MI}	0·5 day^{-1}	
ρ_I	$6{\cdot}0 \times 10^3$ molecule × cell^{-1} × day^{-1}	σ_I	$1{\cdot}0 \times 10^{12}$ M^{-1} day^{-1}	
α_I	24·0 day^{-1}	σ_R	$2{\cdot}0 \times 10^{10}$ M^{-1} day^{-1}	
α_R	1·0 day^{-1}			
Q_{blood}	1·0 l	Q_M	$4{\cdot}0 \times 10^{-4}$ l	
Q_{LALT}	$1{\cdot}2 \times 10^{-2}$ l	Q_{LE}	$6{\cdot}0 \times 10^{-4}$ l	

in the differential subsystems corresponding to IAV-sensitive tissue compartment and to the T lymphocyte or B lymphocyte activation processes, gives the following estimates of the relative growth rates: ~100:1 (compared to ~1:1 for acute hepatitis B case). These numbers make the point that fast non-specific mechanisms play a vital role in limiting the spread of influenza virus during the initial phase of infection, before the specific immune response is able to bring the infectious process under control. The IFN system is considered to be the major mechanism limiting the influenza A infection within the first 2–3 days (Kilbourne, 1987). To make the antiviral immune response model a predictive tool for biologically grounded and practically observed variations in influenza course and severity, it seems necessary to consider explicitly the IFN system by extending the model system of equations. Without explicit description of the IFN system reaction, the predictive ability of our antiviral immune response model with respect to infection severity seems to be seriously limited by the simplified description of the initial phase of IAV infection.

5. Modeling of Interferon Response in Influenza A Virus Infection

In the former part of the paper we have assumed that in uncomplicated infection IAV can destroy only one-third of epithelium cells covering the upper part of the airways. This assumption is called into question by the contradiction between, on the one hand, the high rate of IAV replication, the high cytotoxicity of the virus, the high concentration of the virus in the nasofarengal wash in the acute phase of disease and, on the other hand, the wide spectrum of clinical manifestations of influenza: from minimal damage of epithelium (approximately 60–80% of cases) to serious infection up to a lethal outcome (approximately 1%). Therefore, there must be mechanisms that can provide considerable but variable protection to epithelium cells from person to person (Jackson & Muldoon, 1975; Harris, 1984).

5.1. GENERAL CONSIDERATION

Numerous clinical and experimental observations suggest an important role for interferon in limiting

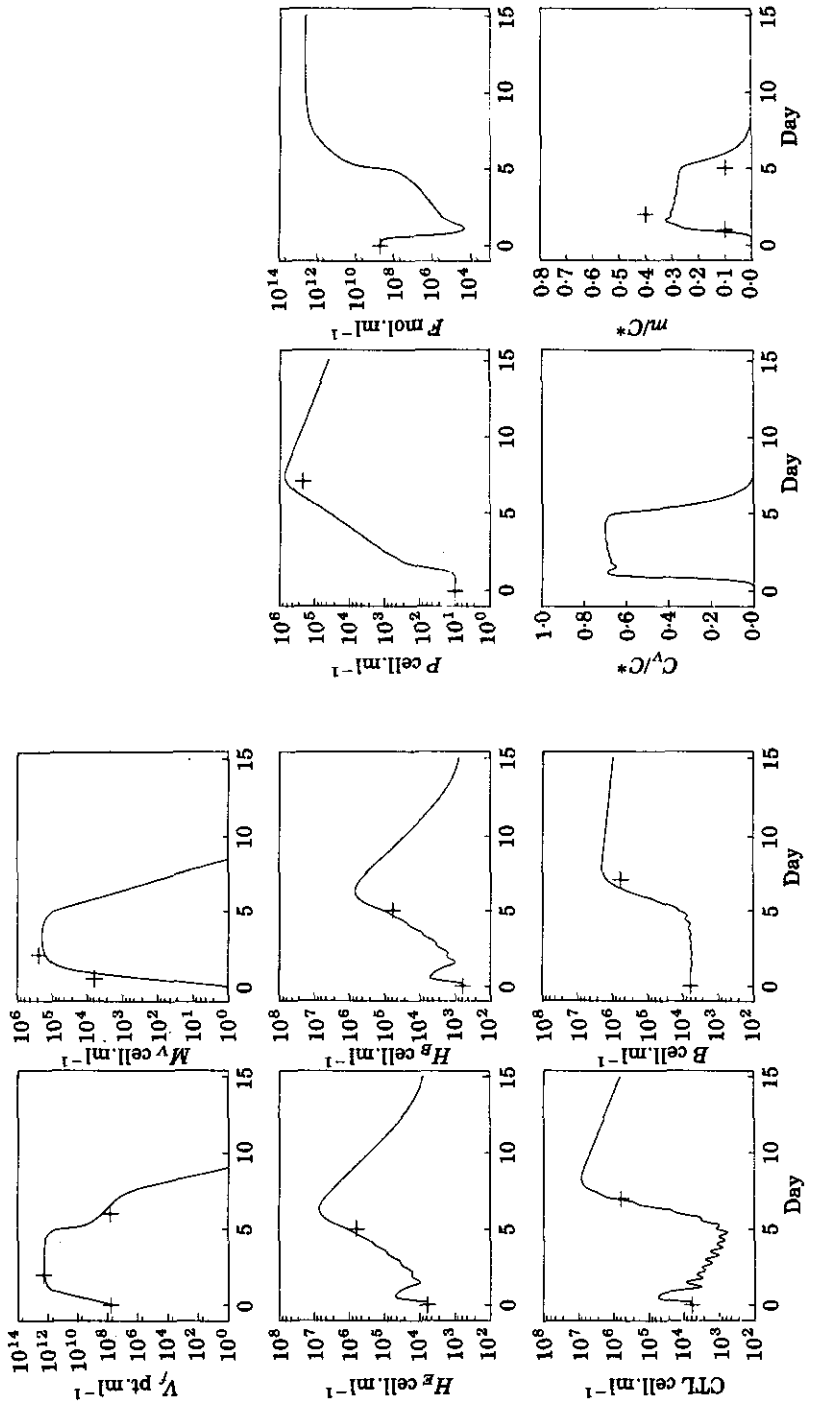

FIG. 4. Solution of the antiviral immune response model simulating the course of uncomplicated influenza A virus infection. Estimated values of model variables, marked by (+) are given according to the generalized picture of uncomplicated influenza A infection. The solid lines are the model solution corresponding to the parameter set given in Table 5. The estimates of several parameters were refined by fitting the model to the generalized picture data.

the virus infection (Zdanov & Bukrinskaja, 1969; Kilbourne, 1987). IFN is the earliest sign of the known host defense mechanism. It is operative within hours after the infection begins. Activation of the IFN system during acute viral infection *in vivo* lasts from several days to 3 weeks (Baron *et al.*, 1981). There is little doubt, at present, that IFN forms the first line of defense against viral infections before the specific immune mechanisms are fully mobilized (Joklik, 1985; Stewart, 1986).

Interferon (or more correctly interferons) are comprised of at least three types of proteins which are newly produced and secreted by body cells stimulated by foreign substances.

Interferon-α and interferon-β (IFN-α and IFN-β) are produced predominantly by leukocytes and fibroblasts, respectively, in response to viral infection or to a variety of inducing agents. Interferon-γ (IFN-γ), formerly called "immune", is produced by unsensitized lymphoid cells in response to mitogens and by sensitized lymphocytes when stimulated with specific antigen. All IFNs possess both antiviral and anticellular activity; all interferons cause interference with the multiplication of viruses and regulate a variety of cellular (including immune cells) functions. In general, it may be said that the effectiveness of inducing antiviral activity differs widely both with the type of cell and the type of IFN (Balkwill, 1986*a*, *b*, *c*).

5.2. CELLULAR COMPOSITION OF UPPER AIRWAYS

First, it should be noted that interferons are characterized by poor diffusion capacity in compact tissue and consequently the local (in the fluid around cells) concentration of IFNs is the major determinant of the degree of antiviral activity (Dianzani *et al.*, 1978).

Epithelial cells are the major component of airway epithelium (more than 90% of the total cell count under normal conditions—see Heino *et al.*, 1990). IAV cause productive infection in these cells and destroy them. Inflammatory cells (less than 10% in the normal case and up to 50% during inflammation) include predominantly lymphocytes and a variable (from 20%–50%) proportion of macrophages (Holt & Schon-Hegrad, 1987; Heino *et al.*, 1990) or essentially macrophages (up to 95–97%—Beasley *et al.*, 1989). IAV cause abortive or weakly productive infection in lymphocytes and macrophages. Infection changes the functional properties of these cells considerably and effectively induces interferon synthesis (Jakab, 1990; Roberts *et al.*, 1979). Although theoretically all nuclear cells are considered as potential produces of interferons in response to virus infection (Isaaks & Lindenmann, 1957), it should be noted that rapidly replicating viruses (such as IAV) are able to block cell protein synthesis at early stage of permissive cell infection (Beloso *et al.*, 1992). Consequently, IFN production in the case of rapidly replicating viruses is determined by non-permissive cells located in the tissue (such as leukocytes infiltrating airway epithelium), and IFN binding to cellular receptors must precede to virus invasion. The important role *in vivo* of leukocytes, and, especially, of macrophages as interferon producers is emphasized in many papers (Borecky *et al.*, 1974; Shwartzman & Chazenson, 1978; Mogensen & Virelizier, 1987).

Let us consider experimental data concerning the kinetics of antiviral protective interferon reaction.

5.3. KINETICS OF INDUCTION OF ANTIVIRAL STATE IN LUNG EPITHELIUM CELLS

Conditionally one may distinguish between direct antiviral activity of IFN (via induction of an antiviral state in cells) and indirect antiviral activity (via the increasing effectivity of other defense mechanisms, mainly the immune system). By its nature the IFN-induced antiviral state is a consequence of the induction of the synthesis of several new proteins in the cell, making it resistant to virus challenge.

The following steps of antiviral state induction have been determined (Joklik, 1985):

- IFN molecules bind to specific high-affinity receptors existing in the cellular membrane. The number of these receptors varies from 10^2–10^4 per cell. IFNs bind with an apparent binding constant of 10^{-10}–10^{-11} M (Balkwill, 1986*a*);
- the IFN–receptor complex is subjected to endocytosis, which occurs within 1–2 hr. Internalized IFN is rapidly degraded;
- internalization triggers a rapid change (in as little as 5 min) in the pattern of mRNA and protein synthesis;
- these proteins (e.g. Mx and related proteins, protein kinase and some others) are the actual effectors of the antiviral state;
- the antiviral state usually lasts for several days (up to 10) and then decays;
- the continuous presence of IFN-α or -β appear to be necessary to maintain the suppression of virus replication.

Let us consider the potential sources and targets of the IFN defense reaction, which plays an essential role in direct antiviral protection during IAV infection.

5.4. KINETICS OF INTERFERON PRODUCTION

Viruses and double-stranded RNA induce IFNs-α and -β, and, in general, α genes are most efficiently induced in leukocytes. Evidence so far indicates that the inducing factor in viruses is double stranded RNA, which is formed during the replication cycle of virus and that one, or only a few, virus particles are sufficient for this process. The kinetics of IFN production in the case of productive infection tends to be the same for most virus infections. IFN production begins approximately 4 hr after infection, reaches a peak when viral protein synthesis is proceeding at its maximal rate, and then declines. IFN-α may be produced by either lymphocytes or monocytes (macrophages in tissue), but there are considerable differences in the antiviral activity exhibited by different IFN-α subtypes from these two cell types. The major ($\approx 50\%$) subtype of IFN-α produced by monocytes has greater antiviral activity (up to ten times) in comparison with other IFN-α subtypes (Goren *et al.*, 1986). In the case of the IAV virus, induction of IFN production in macrophage begins 2 hr after virus internalization (Mogensen & Virelizier, 1987), reaches a peak at 72–92 hr and then declines (Roberts *et al.*, 1979).

5.5. EQUATIONS AND PARAMETERS FOR IFN RESPONSE DURING INFLUENZA A VIRUS INFECTION

Our mathematical model of protective antiviral action of IFN is based on the following assumptions:

- macrophages infiltrating the airway's epithelium are the principal sources of IFN;
- IFN is secreted into the extracellular fluid, where it reacts with the membrane receptors of intact epithelial cells and thereby establishes antiviral resistance. Cells in this state are completely protected from viral infection;
- after decay of the antiviral resistance cells return into their initial intact state.

The first assumption has already been discussed. The second and third assumptions allow to facilitate the description of the fate of a cell in an antiviral state. Simplifying the description of antiviral resistance decay is the aim of the third assumption. *In vitro* experiments demonstrate that after several days in the resistant state a cell shifts to the refractory state, in which even high IFN concentrations do not induce antiviral resistance. Later, the cells restore their ability to maintain antiviral resistance in the presence of IFN. However, taking into account the duration of the acute phase of IAV infection (≈ 7 days) and the short life time of epithelium cells ($\leqslant 7$ days), one may conclude that the refractory state is practically unachievable in the case of influenza.

We also neglect the following possible processes:

- an IFN-protected cell may be infected with a high dose of viruses,
- virus replication in the infected cell may be terminated by a high dose of IFN.

The last simplification is based on two peculiarities of influenza A viruses: high cytopathicity and high rate of replication.

The processes of protective antiviral action of IFN during influenza A virus infection are described by the following variables (see Table 2 for compartment characteristics):

$M_I(t)$—the concentration of IFN producing macrophages in the intercellular spaces of the epithelium layer covering the six upper branching of the airways (in Q_{LEI} compartment) (M);

$I(t)$—the concentration of IFN-α in the Q_{LEI} compartment (IU ml^{-1});

$C_R(t)$—the concentration of epithelial cells protected from viral infection in the epithelium layer of the six upper branching of the airways (in Q_{LE} compartment) (M).

The equations are:

$$dM_I/dt = \gamma_{M_I} V_f (M_I^* - M_I) - \alpha_{M_I} M_I, \quad (11)$$

$$dI/dt = \rho_I M_I - \alpha_I I - \sigma_I I (C^* - C_V - C_R - m), \quad (12)$$

$$dC_R/dt = \sigma_R I (C^* - C_V - C_R - m) - \alpha_R C_R. \quad (13)$$

Equation (11) for the rate of change of the concentration of the IFN producing macrophages M_I describes the induction (first term) and decay (second term) of IFN synthesis in macrophages. The parameter γ_{M_I} characterizes the rate of IFN synthesis induction (see characteristics in Table 6).

The *in vitro* investigations of Dianzani *et al.* (1978) show that at leukocyte concentrations greater than 5×10^6 cells ml^{-1} the IFN synthesis and subsequent antiviral resistance are developed about 1 hr (t_{ind}) after induction. Virus particles (in particular, RNA viruses) are effective inducers of IFN synthesis. Only one viral particle per cell is sufficient for induction of IFN synthesis (Marcus, 1983), and *in vitro* experiments usually are carried out at a multiplicity equal from 1 to 10 viruses per cell. Therefore, the concentration of viruses being equal to the concentration of any cellular elements in epithelium layer is sufficient to induce (V_f^{ind}) IFN synthesis in most macrophages within the time t_{ind}.

TABLE 6
Quantitative characteristics of interferon induction, production and action processes

Name of characteristics	Value (unit)	References
Molecular weight of interferon	17 000 (a.u.)	Joklik (1985)
Specific activity of pure interferon species—weight of international reference unit	2×10^{-12} (g) $\approx 7 \times 10^{7}$ (molecules)	Joklik (1985)
Rate of interferon production by influenza A virus-induced leukocytes (in average)	7×10^{-6}–3×10^{-4} IU/(cell × day) [8×10^{-5} IU/(cell × day) or 6×10^{3} molec/(cell × day)]	Chonmaitree *et al.* (1988)
Duration of interferon production by virus-induced cells	2 (days)	Semenov *et al.* (1982)
Time required for development of anti-viral resistance at different cell concentrations:		Dianzani *et al.* (1978)
5×10^{6} cells ml^{-1}	1 (hr)	
5×10^{4} cells ml^{-1}	4–7 (hr)	
Duration of maintenance of anti-viral resistance	several days	Joklik (1985)
if sufficient IFN conc. is maintained	5–7 (days)	Semenov *et al.* (1982)
Half-life of recoverable interferon after intra-nasal spray:		Scott (1984)
fast decay	20 (min)	
slow decay	1–4 (hr)	

To construct an estimate for the IFN induction rate constant γ_{M_I} we suggest the following scheme, which allows for the characteristics t_{ind} and V_f^{ind} of the IFN synthesis induction process:

$$\gamma_{M_I} = \frac{1}{t_{\text{ind}} \times V_f^{\text{ind}}}.$$

This estimate allows us to describe quantitatively the kinetics of the induction of IFN synthesis in most epithelial macrophages. The concentration of any epithelial cells range from 10^{8}–10^{10} cells ml^{-1} (Table 2), and the concentration of macrophages under normal circumstances (M_f^*) is about 10^{7}–10^{9} cells ml^{-1} (Table 2). Hence, the value of V_f^{ind} ranges from 10^{8}–10^{10} part. ml^{-1} and

$$\gamma_{M_I} \approx 1{\cdot}4 \times 10^{13}\text{–}1{\cdot}4 \times 10^{11}\ \text{M}^{-1}\,\text{day}^{-1}.$$

The parameter α_{M_I} characterizes the kinetics of decrease of IFN synthesis by macrophages M_I in the absence of the inducer (Roberts *et al.*, 1979):

$$\alpha_{M_I} \approx 0{\cdot}5\text{–}0{\cdot}3\ \text{day}^{-1}.$$

Equation (12) for the rate of change of the IFN concentration I describes the processes of IFN synthesis by macrophages M_I (first term), the decrease of IFN concentration due to its natural decay (second term) and the binding to receptors on intact epithelial cells (third term).

The constant ρ_I describes the rate at which IFN molecules are secreted by macrophages M_I into the epithelial intercellular fluid compartment Q_{LEI} (see Tables 2, 6). The rate of IFN secretion by a single cell may be estimated using, for example, the data of Chonmaitree *et al.* (1981) as follows:

$$\rho_I \approx 7 \times 10^{-6}\text{–}3 \times 10^{-4}\ \text{IU (cell} \times \text{day)}^{-1}.$$

The parameter α_I, the IFN decay rate constant, characterizes the rate at which IFN molecules decay in the intercellular space, Q_{LEI}, diffusing in the fluid lining the epithelium (Q_M) and through the basement membrane. In the work of Dianzani *et al.* (1978) an assumption was made that the half-life of IFN in the extracellular fluid is similar to the rapid turnover time in serum, i.e. $t_{1/2} \approx 10$ min. However, from the data presented in (Bocci, 1985), which characterizes IFN pharmacokinetics during intramuscular and subcutaneous injections, one can roughly estimate that the half-life of IFN in extracellular fluid is about 2 hr. In present work we used an intermediate value, i.e. $t_{1/2} \approx 42$ min, and therefore $\alpha_I = 24\ \text{day}^{-1}$.

The parameter σ_I was considered to be the rate constant of IFN molecules binding with specific receptors on the membrane of intact (non-infected, non-protected) epithelial cells. The number of specific high-affinity receptors of IFN varies from 10^{2}–10^{4} per cell. We assumed that the binding of IFN to receptors may be interpreted as irreversible, because within 1 min after binding, IFN molecules are internalized into the cell. If we take into account that less than 50 IFN molecules per cell are sufficient to establish the antiviral state ($N_I^{\text{suf}} = 50$ molecules), and that the volume of the intercellular space per epithelial cell in normal conditions (Q_{LEI_1}) is about 6×10^{-11}–6×10^{-13} ml (Table 2), then an estimate of σ_I may be obtained by the following scheme:

$$\sigma_I \approx \frac{Q_{LEI_1}}{t_{\text{int}} \times N_I^{\text{suf}}}.$$

It should be noted that an IFN concentration of 50 molecules per 6×10^{-11}–6×10^{-13} ml corresponds to 10^{4}–10^{6} IU ml^{-1}. Substituting the estimates for t_{int},

1 min, and for N_I^{suf} we obtain the following range for σ_I: $\sigma_I \approx 10^{10}$–10^{12} M^{-1} day^{-1}.

Equation (13) for the rate of change of the concentration of epithelial cells protected by IFN from viral infection C_R describes the processes of virus resistant state induction in epithelial cells (first term) and the decay of this state in the absence of sufficient IFN concentration (second term).

The parameter σ_R, the rate constant of induction of the virus resistant state in epithelial cells, phenomenologically characterizes the kinetics of intact epithelial cells transition to a virus resistant state, directed by intercellular IFN. The time for this transition $t_{C\to C_R}$, is about 1 hr (see Table 6). To describe the induction of the antiviral state in a majority of epithelial cells, it is necessary to estimate the sufficient concentration of IFN (I^{suf}). The IFN is a very efficient cellular hormone and moderately elevated amounts of IFN (about 10^1–10^2 IU ml^{-1}) are sufficient to develop significantly elevated antiviral resistance (Dianzani *et al.*, 1978). To describe the induction of antiviral resistance in the time $t_{C\to C_R}$ in about C^* epithelial cells we evaluated I^{suf} by the value N_I^{suf}.

An estimate of antiviral resistance induction rate constant was derived from the following scheme:

$$\sigma_R = \frac{1}{t_{C\to C_R} \times N_I^{suf}}.$$

Substituting in this expression one obtains $\sigma_R \approx 2 \times 10^{10}$ M^{-1} day^{-1}.

The parameter α_R, the rate constant of decay of the epithelial cell's virus resistant state, characterizes the process of transition of the protected epithelial cells to the virus permissible state in the absence of intercellular IFN. The time for this transition, $t_{C_R\to C}$, is about 1 day (Joklik, 1985), so that $\alpha_R = 1$ day^{-1}.

Thus we have elaborated the estimates for the system of equations for the IFN response submodel.

To account for the antiviral protection of epithelial cells by IFN, minimal modifications in eqns (1) and (2) should be made:

$$dV_f/dt = \nu C_V + nb_{CE}C_V E - \gamma_{VF}V_f F f_V(I) - \gamma_{VM}V_f - \gamma_{VC}V_f(C^* - C_V - C_R - m) \quad (14)$$

$$dC_V/dt = \sigma V_f(C^* - C_V - C_R - m) - b_{CE}C_V E f_C(I) - b_m C_V \quad (15)$$

Extending the antiviral immune response model eqns ((14), (15), 3–10) by the IFN submodel eqns (11–13), with the parameters given in Table 5 we obtain a more detailed and adequate model of defense processes during IAV infection. The corresponding solution is presented on Fig. 5. The correlation with the GP data seems to be satisfactory. Therefore, the model [eqns (14), (15) (3–13)] may be considered as a descriptive tool consistent with the general short-term regularities of both the antigen-specific immune response and the non-specific IFN response during IAV infection. This model is exploited in the next sections to make quantitative predictions, which are open to direct interpretations and comparison with observations.

6. Quantitative Predictions of the Influenza Infection Model

6.1. Immune protection of susceptible individuals

The immune protection of susceptible individuals against subsequent infection is defined by the ability of an adaptive immune response to generate immunological memory. The generation of immunological memory has been shown in some viral infections to involve proliferation of precursor cells to form large numbers of both T and B memory cells, but the mechanisms involved in this process are still not well understood (Ada, 1991).

The host's immune response to IAV is particularly important in limiting the severity and duration of illness as well as in protecting against subsequent infection by an antigenically similar influenza strain (Leigh *et al.*, 1991). It was clearly established that the general pattern of antibody response to IAV infection is similar to that of primary infections by other viruses and is characterized by stable elevated levels of systemic IgG and local IgA for at least 2–3 years after infection. Resistance to reinfection has generally been attributed to the presence of HA-specific Ab in serum or in respiratory airways secretions, and it appears that the presence of sufficient Ab at either site is capable of conferring resistance (Welliver & Ogra, 1988).

Generally, cytotoxic T cell responses develop in man following IAV or immunization. These responses exhibit the capability of providing protection against subsequent influenza virus infection, even when virus-specific serum Ab is absent (Welliver & Ogra, 1988). The half-life of influenza human CTL memory has been estimated to be 2–3 years (Mitchell *et al.*, 1985; Murphy & Webster, 1985). It is believed that long-lasting protection is provided only by Abs and by B cell memory of the correct Ig class and location (Zinkernagel *et al.*, 1985). Whether Abs alone are sufficient for protection against reinfection, or whether memory CTLs are also required, is not yet clear.

Realistic ranges for an increase in the precursor frequency of B and T cells providing protection

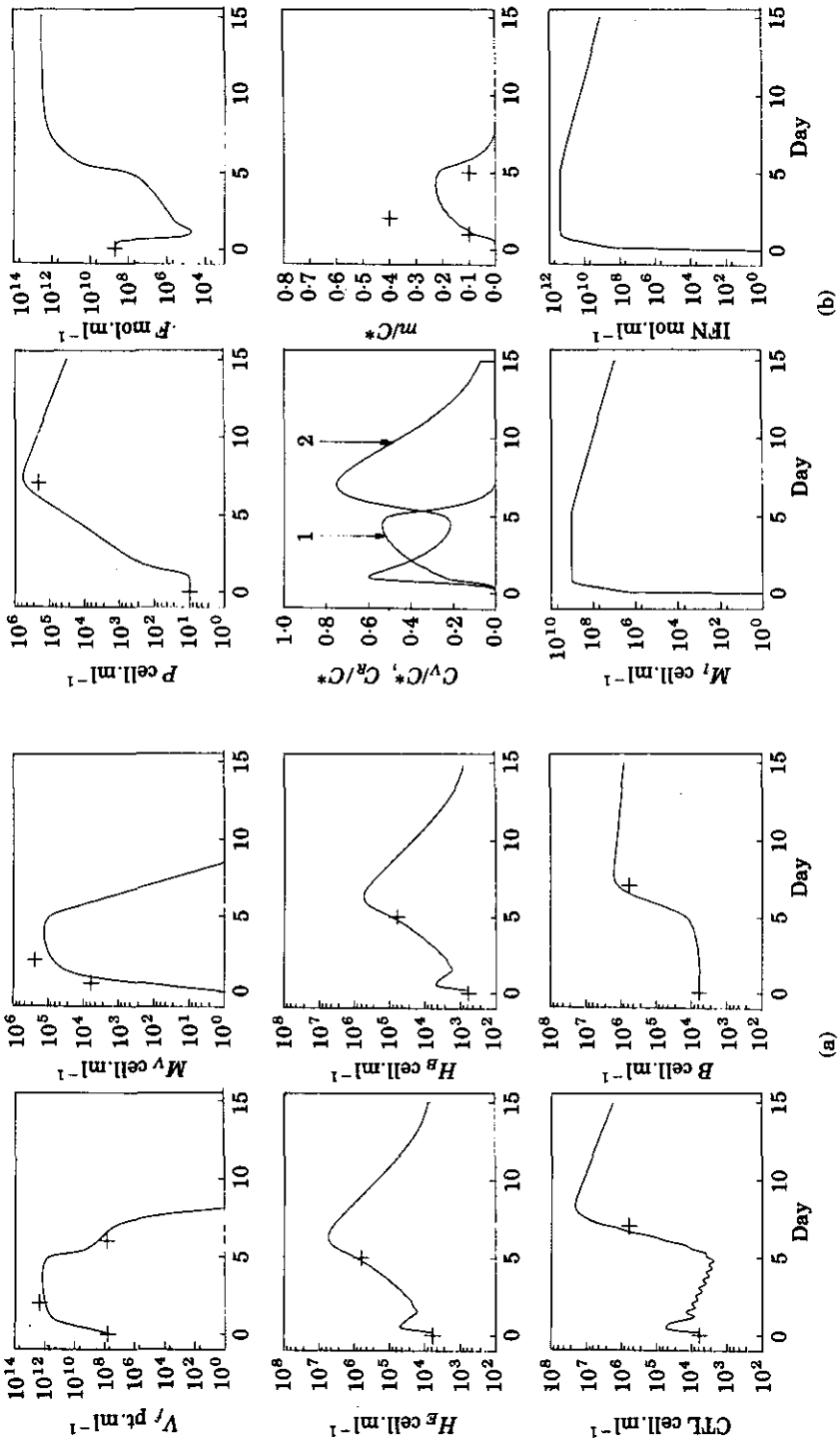

FIG. 5. The solution of coupled antiviral immune response–interferon response model simulating the course of uncomplicated influenza A virus infection. The data of the generalized picture of the infection are marked by (+). The solid lines are the model solution corresponding to the entire parameter set of Table 5. The concentration units are referred to three basic compartments: LALT, mucous and lung epithelium. Arrows (1) and (2) denote C_V/C^* and C_R/C^*, respectively.

against reinfection with the same virus may be assessed by analyzing the reports on immunization against influenza. The main difficulties in deriving estimates are the critical dependence of the effect on the type of vaccines, the recipient's prior antigenic experience and the route of adminstration (Tyrrel, 1980; Murphy *et al.*, 1982; Ada & Jones, 1986; Sullivan *et al.*, 1990; Ada, 1991). In Sullivan *et al.* (1990) it is reported that Ab titers 3 weeks after vaccination with inactivated influenza vaccines paralleled the antigen content of the vaccines, and the observed rises in hemagglutination-inhibition serum Ab titers were 4 to 32-fold. However, the inactivated influenza virus vaccines do not provide complete protection. Generally, vaccination with live, attenuated, cold-adapted IAV viruses efficiently stimulates both systemic and local Ab responses. The serum and secretory HA antibody levels of young vaccinated children were found to increase 30–10^3-fold (Murphy *et al.*, 1982).

In studies with human volunteers at the Common Cold Center, cytotoxic T cell memory correlated with rapid clearing of administered virus in individuals with no antibody immunity. The observations concern individuals, who have protective levels of CTL (Mitchell *et al.*, 1985). However, one should differentiate the different sense of protection used: protection against illness and protection against infection. The memory CTLs that have been characterized after infection or vaccination of humans have a cross-reactive pattern of cytotoxicity. A similar estimate of memory T cell may be assessed from data on T cell precursor frequency increase after influenza infection; a 10–100-fold elevation seems to be a reasonable range.

The above phenomenology of immune protection of susceptible individuals was used to analyze the quality of corresponding model predictions. The mathematical model of IAV infection has an "uninfected" steady state, $x_{st}(t)$:

$$x_{st}(t) = [0,0,H_E^*,H_B^*,E^*,B^*,P^*,F^*,0,0,0,0,0],t \in R,$$

characterized by zero values of the viruses and infected cells. This steady state corresponds to the state of an individual in the absence of antigen.

An infection with IAV may be considered as a perturbation from equilibrium corresponding to the uninfected state x_{st}. The individual may be susceptible to or protected against IAV infection. Protection means that the introduction of a small amounts of IAV, perturbing the uninfected state, does not cause the progression of infection. In other words, the steady state should be stable with respect to small perturbations in the first component of the steady-state vector x_{st}. The susceptible state of an individual is characterized by sensitivity to invasion of IAVs, and, correspondingly, the uninfected steady state x_{st} should be unstable to small perturbations in V_f.

The condition for stability of x_{st} with respect to V_f-perturbations follows from that for the asymptotic stability of x_{st}. A sufficient condition for the asymptotic stability of x_{st} can be easily obtained by linear stability analysis. The Jacobian matrix for the linearized differential system has eigenvalues which are all negative if the following inequality holds (the parameters $\alpha_M, \alpha_H^{(E)}, \alpha_H^{(B)}, \alpha_E, \alpha_B, \alpha_P, \alpha_F, \alpha_m, \alpha_{M_1}, \alpha_I, \alpha_R$ are assumed to be positive):

$$(\gamma_{VF}F^* + \gamma_{VM} + \gamma_{VC}C^*)(b_{CE}E^* + b_m) > v\sigma C^*.$$

It is independent of delays for the zero steady state x_{st}. The parameters on the left-side of the inequality characterize the virus neutralization and infected cells destruction processes, while those on the right-side—the growth rates in virus—infected cell system. Thus, the inequality gives the threshold condition for immune protection to infection with a small number of influenza viruses. Notice, that the humoral and cellular immunity parameters appear in the inequality in a multiplicative way.

Substituting the parameters corresponding to IAV infection into the stability condition one can easily find that the parameters of Table 5 correspond to susceptible individuals, because one eigenvalue is positive. To ensure the asymptotic stability of the uninfected steady state x_{st} (wherein all eigenvalues of the Jacobian matrix have negative real parts) the concentrations of IAV specific Abs or CTLs should be increased with respect to the particular values F^* and E^* from Table 5. Elevated concentrations of IAV-specific Abs and CTLs which ensure the stability condition transform an individual from a susceptible to a protected state. These protective levels of Abs and CTLs are denoted by (F_{prot}) and (E_{prot}), respectively. The pattern of increasing may be different: if only the humoral chain is considered, then $F_{prot}/F^* \approx 150$; if only the CTL chain is considered, then $E_{prot}/E^* \approx 740$; however, the joint rise of humoral and CTL components requires only 50-fold excess: $F_{prot}/F^* \approx E_{prot}/E^* \approx 48$, to meet the stability condition. One can see that these estimates qualitatively agree with the ranges of the IAV-specific immunity parameters, like the frequencies of antigen-specific immunoglobulins and effectors, elicited by immunization to provide protection of susceptible individuals.

The protective performance of the estimated Ab and CTL levels (F_{prot}) and (E_{prot}) needs to be further clarified. The asymptotic stability concept considers arbitrarily small perturbations of the steady states, and it would be interesting to assess the attraction domain of the steady state x_{st} with respect to finite perturbations in the first component V_f^{st}. This would represent the stability of the uninfected state with respect to infection with large doses of viruses. We have studied this property of x_{st} numerically using the parameter values of Table 5, except for the values of E^*, B^*, P^*, F^*, which were taken 50-fold greater to ensure the stability condition.

The problem for simulation is the following:

- an "immune" organism with protective levels of Abs, plasma cells, B cells and CTLs $F_{prot} = 50 \times F^*, P_{prot} = 50 \times P^*, B_{prot} = 50 \times B^*, E_{prot} = 50 \times E^*$, where F^*, P^*, B^* and E^* are from Table 5, is challenged with V_f^0 influenza A viruses;
- V_f^0 is varied in the range $1–10^{12}$ vir. ml^{-1}.

It is known that resistance induced by immunization is manifested by a reduction in the frequency and severity of the illness in vaccinated individuals compared with controls, but protection is not complete. We suggest that correct estimates of the model parameters would provide a realistic range for IAV inoculum size that may be coped with efficiently by a protectively immunized individual. We investigated the dependence of solution behavior with respect to an increasing initial dose of viruses V_f^0 to find out the size of inoculum which breaks through the immune barrier and develops the disease.

In Fig. 6(a) we display the virus component of the computed solutions, simulating the result of infection of a protected host when the initial IAV concentration is varied ten orders of magnitude. It was found that for V_f^0 (the concentration of viruses in the mucous compartment at time t_0) in the range $1–10^8$ vir. ml^{-1} a 50-fold rise in specific Abs, B cells, P cells and CTLs prevents development of the disease. This may be interpreted as immune protection of individuals. Higher concentrations of $V_f^0 \geq 10^9$ vir. ml^{-1} may induce disease, with a severity and duration depending on the reactivity of the immune system. Indeed, higher concentrations of helper T cells [Fig. 6(b)] lead to a decrease in duration and severity of infection [compare with Fig. 6(a)]. Numerical investigations show that the upper size of inoculum V_f^0 which may be efficiently coped with by an immunized individual is related to the excess of actual levels of antibodies and CTLs with respect to those providing equality to 1 in the stability threshold condition. Thus, we can conclude that the set of identified parameters qualitatively agrees with the phenomenology of immunization procedures.

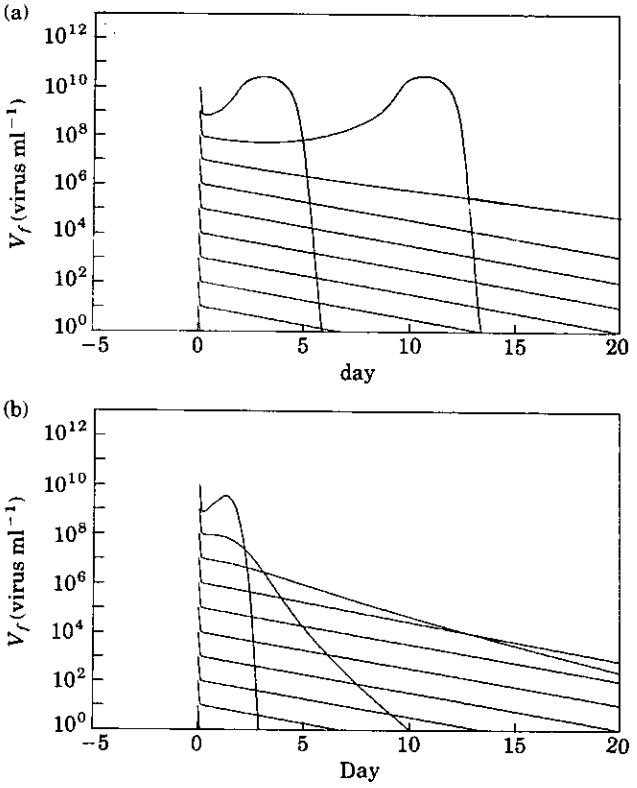

FIG. 6. Modeling of immune resistance to challenge with various influenza A virus doses. The administered to mucous compartment dose of influenza A viruses $V_f(0)$ ranges from $10–10^{10}$ vir. ml^{-1}. (a) The homeostatic concentrations of antibodies, B cells, plasma cells and CTLs to the virus are taken 50-fold greater than in Table 5 to be sufficient for protection of susceptible individuals against "small" doses of influenza A viruses. It may be seen that an inoculum size in the range $1–10^8$ vir. ml^{-1} can be eliminated without the need for specific immune response. A higher initial concentration of viruses ($> 10^9$ vir. ml^{-1}) may induce disease with the severity and duration depending on parameters influencing the reactivity of the immune system. (b) In parallel with the 50-fold increase in steady state levels of Abs, B cells, plasma cells and CTLs, the concentrations of influenza-specific helper T-cell subsets (Th1, Th2) has been taken 50-fold greater than in Table 5. The higher levels of Th1 and Th2 cells lead to an obvious decrease in severity of infection for $V_f^0 > 10^9$ vir. ml^{-1}, compare (a) and (b).

6.2. CUMULATIVE CONTRIBUTION TO THE INFECTION COURSE FROM UNDERLYING PROCESSES

The model-based analysis of the balance between particular processes described in the model during the course of an acute IAV infection stems from considering the values of auxiliary variables, which are the quadratures of selected terms on the right-hand side of the model differential system over the disease interval.

Let us examine a number of selected cumulative characteristics of infection, relating them with the model equations in the following way:

- $V^C = \int_0^T \nu C_V dt$—the total amount (t.a.) of IAVs secreted by infected epithelial cells during the time T of infection;
- $V^F = \int_0^T \gamma_{VF}(1 + \mu_{VF} C_V) F V_F dt$—t.a. of IAVs neutralized due to the inflammation-augmented effect of IAV-specific antibodies;
- $V^M = \int_0^T \gamma_{VM} V_f dt$—t.a. of IAVs removed from the respiratory tract owing to nonspecific clearance mechanisms;
- $V^{C \to C_V} = \int_0^T \gamma_{VC}(C^* - C_V - C_R - m) V_f dt$—t.a. of IAVs spent on infection of epithelial cells;
- $C^V = \int_0^T \sigma (C^* - C_V - C_R - m) V_f dt$—t.a. of virus-infected epithelial cells;
- $C^R = \int_0^T \sigma_R (C^* - C_V - C_R - m) I dt$—t.a. of IFN-protected epithelial cells;
- $C^E = \int_0^T b_{CE}(1 + \mu_{CE} C_V) E C_V dt$—t.a. of virus-infected epithelial cells destroyed by inflammation-augmented action of specific CTLs;
- $C^m = \int_0^T b_m C_V dt$—the cumulative cytopathic effect of IAV;
- $F^P = \int_0^T \rho_F P dt$—t.a. of IAV-specific antibodies produced during infection;
- $F^V = \int_0^T \gamma_{FV} V_f F dt$—t.a. of IAV-specific antibodies utilized for neutralization of viruses;
- $E^{\text{new}} = \int_0^T \xi(m)(\rho_E - 1)(M_V H_E E)|_{t-\tau_E} dt$—t.a. of IAV-specific CTLs born owing to clonal expansion;
- $E^{\text{div}} = \int_0^T b_p^E [M_V(t) H_E(t) - M_V(t - \tau_H^E) \times H(t - \tau_H^E)] dt$—t.a. of CTLs in the division process at time T;
- $E^{C_V} = \int_0^T b_{EC} C_V E dt$—t.a. of IAV-specific CTLs utilized in the process of infected cells destruction;
- $B^{\text{new}} = \int_0^T \xi(m) b_p^B (\rho_B - 1)(M_V H_B B)|_{t-\tau_B} dt$—t.a. of IAV-specific B cells born owing to clonal expansion;
- $P^{\text{new}} = \int_0^T \xi(m) \rho_P b_p^P (M_V H_B B)|_{t-\tau_P} dt$—t.a. of IAV-specific plasma cells born owing to clonal expansion;
- $IFN^M = \int_0^T \rho_I M_I dt$—t.a. of IFN produced;
- $IFN^C = \int_0^T \sigma_I I (C^* - C_V - C_R - m) dt$—t.a. of IFN molecules utilized for the protection of IAV-sensitive epithelial cells.

The characteristic values (rounded off to one digit) in physical units for three different observation times are given in Table 7. The following conclusions can be drawn from the balance analysis of the influenza A infection model:

- the contributions of inflammation-augmented IAV-specific antibodies and physical clearance mechanisms to the neutralization of viruses are much the same and about 50-fold greater than from the adsorption of IAV during the infection of sensitive epithelial cells;
- the cytopathic effect of IAV upon infected epithelial cells is the dominant factor accounting for about 85% of tissue destruction;

TABLE 7

Balance analysis of separate processes described in the model for the dynamics of uncomplicated influenza A virus infection

Variable	3rd day	7th day	14th day	Unit
V^C	$0{\cdot}4 \times 10^{13}$	10^{13}	10^{13}	*IAV* particle ml^{-1}
V^F	$0{\cdot}9 \times 10^{11}$	$0{\cdot}4 \times 10^{13}$	$0{\cdot}4 \times 10^{13}$	in mucous
V^M	$0{\cdot}3 \times 10^{13}$	$0{\cdot}7 \times 10^{13}$	$0{\cdot}7 \times 10^{13}$	compartment
$V^{C \to C_V}$	$0{\cdot}6 \times 10^{11}$	10^{11}	10^{11}	
C^V	$0{\cdot}2 \times 10^{11}$	$0{\cdot}4 \times 10^{11}$	$0{\cdot}4 \times 10^{11}$	epithelial cells ml^{-1}
C^R	$0{\cdot}1 \times 10^{11}$	$0{\cdot}3 \times 10^{11}$	$0{\cdot}6 \times 10^{11}$	in mucous
C^m	$0{\cdot}1 \times 10^{11}$	$0{\cdot}3 \times 10^{11}$	$0{\cdot}3 \times 10^{11}$	compartment
C^E	$0{\cdot}3 \times 10^{10}$	$0{\cdot}6 \times 10^{10}$	$0{\cdot}6 \times 10^{10}$	
F^P	$0{\cdot}2 \times 10^{10}$	10^{12}	$0{\cdot}5 \times 10^{13}$	anti-HA molecules ml^{-1}
F^V	$0{\cdot}3 \times 10^{10}$	10^{11}	10^{11}	in mucous, blood, lymph
E^{new}	$0{\cdot}2 \times 10^{6}$	10^{7}	10^{7}	IAV-specific T cell ml^{-1}
E^{div}	$0{\cdot}2 \times 10^{6}$	$0{\cdot}8 \times 10^{7}$	0	in LNs of LALT
E^{C_V}	$0{\cdot}2 \times 10^{5}$	$0{\cdot}6 \times 10^{5}$	$0{\cdot}6 \times 10^{5}$	compartment
IFN^M	$0{\cdot}1 \times 10^{14}$	$0{\cdot}4 \times 10^{14}$	$0{\cdot}4 \times 10^{14}$	molecules ml^{-1}
IFN^C	$0{\cdot}7 \times 10^{12}$	$0{\cdot}2 \times 10^{13}$	$0{\cdot}3 \times 10^{13}$	in mucous compartment
B^{new}	$0{\cdot}4 \times 10^{4}$	$0{\cdot}2 \times 10^{7}$	$0{\cdot}2 \times 10^{7}$	IAV-specific cell ml^{-1}
P^{new}	$0{\cdot}2 \times 10^{4}$	$0{\cdot}7 \times 10^{6}$	$0{\cdot}9 \times 10^{6}$	in LNs of LALT compartment

- throughout the influenza infection the amounts of virus particles produced, specific antibody molecules secreted and IFN molecules are in the ratio $1:10^3:10$;
- throughout the influenza infection the numbers of infected epithelial cells, IFN-protected epithelial cells and clonally expanded CTLs are in the ratio $1:1{\cdot}5:0{\cdot}06$;
- all through the IAV infection about 2×10^7 B lymphocytes and 10^7 plasma cells are born due to the clonal selection and expansion; thus the average differentiation index is about 0·3;
- about 4×10^{10} infection-damaged epithelial cells are eventually regenerated;
- the number of activated lymphocytes, in their division cycle, changes dynamically with respect to that of G_0/G_1-phase lymphocytes with the peak ratio about 2:1.

We suggest that at the level of cumulative balances the estimates of parameters for uncomplicated IAV infection (Table 5) are qualitatively correct except for that of b_{EC}. Indeed, during the infection the estimated number of infected epithelial cells destroyed directly by CTL killing is about 5×10^{-13} M, while the number of CTL spent was 10^{-16} M. This gap is related to our oversimplified description of the CTL population as multifunctional and/or homogeneous (able to proliferate and kill simultaneously) (for another approach see Sidorov & Romanyukha, 1992). So, if one would like to trace correctly the time course of CTLs, they need to be subdivided into, at least, two subsets: one being related to the proliferation processes in the LN compartment, and the other performing the cytolytic action in the sensitive tissue compartment (like B cells and antibodies in the humoral part of the model). However, in this influenza A model we focus our attention primarily on CTL kinetics in the LNs and regard the concentration of mature CTLs in the sensitive tissue as proportional to that in LNs. Thus we underestimate the value of b_{EC} by 50–100 times, but keep the kinetics of CTL proliferation in LN correct. However, refined estimation needs more careful data on the balances of the basic processes.

An important conclusion which can be drawn from the above analysis is the fundamental role of nonspecific defense mechanisms (IFN system, physical clearance mechanisms, inflammation and cytopathic action of viruses in influenza infection dynamics.

6.3. SENSITIVITY OF THE MODEL TO PERTURBATIONS OF PARAMETERS

The aims of sensitivity analysis with respect to small random perturbations of the basic parameters set (Table 5) are the following:

- to explore how robust the developed influenza model is in relation to noisy parameter values;
- to study the sensitivity scale of selected solution characteristics to random parameter variations.

The solutions of both problems would help in an examination of the determinants of observed population heterogeneity in influenza severity during epidemics.

To attack the questions we selected several solution-derived characteristics which have direct biological interpretations and may be considered as criteria for disease severity and for the magnitude of immune response. Generally, an assessment of influenza virus pathogenicity is based upon criteria that include, among others, the level and persistence of upper respiratory tract infection, the magnitude and duration of fever, the frequency and amount of virus shedding, clinical surveillance, etc (Sweet & Smith, 1980). Within the frameworks offered by the model these may be generalized into the following characteristics of disease severity and duration:

$$m_{\max} = \max_{0 \leqslant t \leqslant T}[m(t)];\ \Delta T_{\text{illness}} = T_2 - T_1,$$

where for

$$T_1 \leqslant t \leqslant T_2\ V_f(t) \geqslant 0{\cdot}5 \times 10^{10}\ \text{vir. ml}^{-1};$$

$$V_{f_{\text{total}}} = \int_0^T \nu C_V(t)\,dt,$$

$$m_{\text{total}} = \int_0^T [b_m C_V + b_{CE}(1 + \mu_C C_V/C^*)C_V E]\,dt.$$

The value $V_f(t) \approx 0{\cdot}5 \times 10^{10}$ vir. ml^{-1} was considered to be the threshold point for the onset of fever, resulting from interaction of IAV with phagocytes in the upper airways and release of leukocyte pyrogen into the blood stream.

The cumulative functions $V_{f_{\text{total}}}$ and m_{total} provide an opportunity to estimate the variation of fever as well as of toxic effects exerted by influenza viruses on epithelial cells. To measure the sensitivity of the specific immune response, we considered the values E_{new}, P_{new}—the total amounts of CTLs and plasma cells generated due to clonal expansion during IAV infection, and the times t_H, t_E, t_P, required for helper T cells, CTLs and plasma cells to increase 10-, 10-, and 10^3-fold, respectively, in response to virus stimulation (t_H: $H_E(t_H) = 10 \times H_E^*$, etc). The latter are related to the immune reaction kinetics (reactivity potential) of IAV specific lymphocyte clones.

Our approach to investigate sensitivity was based on estimating the effect of small random simultaneous perturbations in the values of all parameters (considered as independent variables) on variations of the above introduced model solution characteristics (considered as response variables). For generating random

TABLE 8

Results of stochastic sensitivity analysis for severity characteristics m_{max}, m_{total}, $V_{f_{total}}$, *and the duration of illness,* $\Delta T_{illness}$, *with respect to model parameter perturbations. The parameter* ϵ *is the relative deviation (range for the noise) being added to model parameters. Only those parameters are displayed which influence the characteristics to a considerable extent* ($\geqslant 10\%$)

Index	ϵ	C^*	v	α_m	b_m	α_l	α_M	τ_H^B	ρ_H^B	ρ_B	b_p^P
m_{max}	0·01	53		23	13						
	0·1	50		22	13						
	0·5	37				11					
m_{total}	0·01	48				11					
	0·1	46				10					
	0·5	29				10					
$V_{f_{total}}$	0·01	40	36								
	0·1	38	34								
	0·5	21	25								
$\Delta T_{illness}$	0·01		16				20	11	23	20	10
	0·1		17				19	11	23	18	11
	0·5		10								

numbers we used the IMSL routines GGUBS—a basic uniform (0,1) pseudo-random number generator, and GGNML—a normal or Gaussian random deviate generator. An analysis of regression models, for introduced functionals, including calculation of the percentage of variation of the response variable explained, was performed using the RLSEP routine.

Let α_i, $i = 1,2,\ldots, L\,(L = 48)$, denote the basic values of model parameters, including delays and V_f^0. A series of $N = 100$ calculations of the initial value problem for the model system [eqns (14), (15), (3–13)] DDE over a time interval of 0–20 days with randomly perturbed values of parameters $\alpha_{i,j+1} = \alpha_i(1 + \xi_{i,j+1})$, $i = 1,2,\ldots, L, j = 1,2,\ldots, N$, were carried out. Here, $\xi_{i,j}$ a uniformly distributed on $[-\epsilon,\epsilon]$ random variable has a zero mean $E(\xi_{i,j}) = 0$ and range ϵ. (For normally distributed random variables $\xi_{i,j}$ with mean $E(\xi_{i,j}) = 1$ and dispersion $D(\xi_{i,j}) = \epsilon^2$, the model of parameter perturbation was correspondingly $\alpha_{i,j+1} = \alpha_i \times \xi_{i,j+1}$). We performed a full-scale analysis in the case of uniform perturbations for $\epsilon = 0{\cdot}01$; 0·1; 0·5 and in the case of normal perturbations for $\epsilon = 0{\cdot}01$.

TABLE 9

Results of stochastic sensitivity analysis for characteristics of the reactivity potential of IAV-specific lymphocyte clones—E_{new}, $t_{E=10\times E^*}$, $t_{H_E=10\times H_E^*}$, P_{new}, *and* $t_{P=10^3\times P^*}$, *with respect to model parameter perturbations. The parameter variation scheme is the same as Table* 8

Index	ϵ	v	τ_E	ρ_E	ρ_H^B	ρ_B	α_M	τ_H^E	ρ_H^E	τ_H^B	b_p^P
E_{new}	0·01		33	60							
	0·1		28	40							
	0·5										
$t_{E=10\times E^*}$	0·01				24	17					
	0·1		11	38	21	13					
	0·5										
$t_{H_E=10\times H_E^*}$	0·01	32					13	36	33		
	0·1	33					12	35	34		
	0·5	10					11				
P_{new}	0·01	22			15	16	41				
	0·1	18			13	17	36				
	0·5										
$t_{P=10^3\times P^*}$	0·01	39			13		19			14	13
	0·1	42			11		18			12	14
	0·5										

A summary of results is given in Tables 8 and 9. Only parameters responsible for at least 10% of response variable variation are displayed. It turns out that the characteristics of disease severity $m_{\max}$, m_{total}, $V_{f_{\text{total}}}$ are influenced to the largest extent by C^*—the total amount of epithelial cells in the upper airways susceptible to IAV infection. In Sweet & Smith (1980) a similar point was considered to explain the higher influenza severity in neonates and infants. It was stressed that host and environmental factors may affect the chance of successful contact between virus and respiratory tract cells leading to infection. The host factors include variations in thickness, flow rate and viscosity of mucus and gaps in the blanket, while the environment affects mucus secretions and ciliary action by changes in temperature, ion concentration and air humidity. The replication rate v, cytopathicity parameter b_m and regeneration rate α_m are the other virus and target organ characteristics that strongly influence $V_{f_{\text{total}}}$ and $m_{\max}$. The variations of the IFN system parameter α_I (rate of IFN decay) moderately influence variations of the maximal numbers of destroyed epithelial cells and, correspondingly, the possibility of a fatal outcome.

The mean value for $m_{\max}$ slightly increased from 0·23 to 0·25 when the noise level ϵ rose from 0·01 to 0·5, while that of m_{total} decreased from 3·9 to 3·6.

The duration of the illness $\Delta T_{\text{illness}}$ is influenced dominantly by a group of parameters related to activation of humoral immune response. The magnitude of CTL response (E_{new}) is most sensitive to variations in effector T cell proliferation parameters τ_E and ρ_E. A similar dependence is observed in the case of the humoral response characteristic (P_{new}). The growth rates of cellular and humoral response are sensitive to proliferation parameters, the decay rate of antigen-presenting macrophages and, surprisingly, the virus replication rate v (see Table 9).

The sensitivity structure, generally, is destroyed by large-amplitude noise ($\epsilon \sim 0{\cdot}5$) in parameter values, and remains qualitatively the same for normally distributed perturbations of small amplitude. The model solutions for three selected amplitudes of noise ($\epsilon = 0{\cdot}01$; 0·1; 0·5) qualitatively retained the features of the severity and duration. We could thus conclude that the robustness of the influenza model is satisfactory. A more general and speculative conclusion is that the observed heterogeneity in influenza infection during epidemics may be related to moderate variations in virus–target organ characteristics and more substantial variations in immune responsiveness.

6.4. REGULAR VARIATIONS OF PARAMETERS AND INFLUENZA INFECTION SEVERITY

The basic set of parameter values (Table 5), consistent with the GP data on IAV infection, was examined by studying the effect of deterministic variations of selected parameters over an admissible range on certain characteristics of the immune response and of the disease, which were introduced in the previous two subsections. A one-dimensional variation ($\alpha_i = \alpha_i^* \times \epsilon$, $\epsilon \in [\epsilon_{\min}, \epsilon_{\max}]$) approach was utilized to make the effect clear. The most informative characteristics of the model solution related directly to influenza severity and duration turned out to be the m_{total} and the $\Delta T_{\text{illness}}$. The values of these indices as functions of parameters v, σ, γ_{MV}, C^* and ρ_I are displayed in Fig. 7. It was found that the rise in IAV replication rate v, with respect to the basic value, makes the virus infection more severe for the host. The total number of viruses, destroyed epithelial cells as well as the magnitude of immune response in terms of E_{new}, $E_{\max}$, P_{new}, $P_{\max}$ grow with the increase in v, thus making the infection load to the host more severe. However, the IFN response in terms $IFN_{\max}$ and IFN_{total} turned out to be independent of the variation of the ratio v/v^* in the interval $0{\cdot}1 \leqslant (v/v^*) \leqslant 10$. The low values of replication rate lead to a "persistence" regime ($V_{f_{\min}} > 1$ pt. ml^{-1}) over the considered 3 week interval. The same effect of parameter variation was established for the infection rate σ of sensitive epithelial cells. One can see, however, decreasing values of $E_{\max}$ and E_{new} and practically constant values of $V_{f_{\text{total}}}$ and $\Delta T_{\text{illness}}$ when the ratio of (v/v^*) rises over the 1–10-fold interval.

An increase in C^*—the amount of epithelial cells susceptible to IAV infection, over the range C^*_{basic}–$10C^*_{\text{basic}}$, where C^*_{basic} is equal to C^* from Table 5, leads to a considerable rise in $V_{f_{\text{total}}}$, m_{total} and P_{new}. The values of $\Delta T_{\text{illness}}$ and E_{new} drop, whenever $IFN_{\max}$ remains stable. However, if C^* is 10-fold lower than C^*_{basic}, a persistence regime is established due to weak antigenic signal insufficient for stimulating IAV-specific lymphocyte clones.

The antigen-presenting macrophage stimulation rate, γ_{MV} characterizing the sensitivity to IAV antigens, was varied in the range $10^{-2} \leqslant (\gamma_{MV}/\gamma^*_{MV}) \leqslant 10^2$. It was established that the 1 to 10^2-fold increase in the value of parameter γ_{MV}, causes an amplification of the specific cellular and humoral response leading to a drop in $\Delta T_{\text{illness}}$ and m_{total}. The IFN response remains almost invariant in terms of $IFN_{\max}$ or IFN_{total}. However, a 10-fold drop in γ_{MV} value leads to virus persistence.

The effect of 10^{-2} to 10^2-fold variations in helper T cell homeostatic concentrations (H^*_E and H^*_B) is the

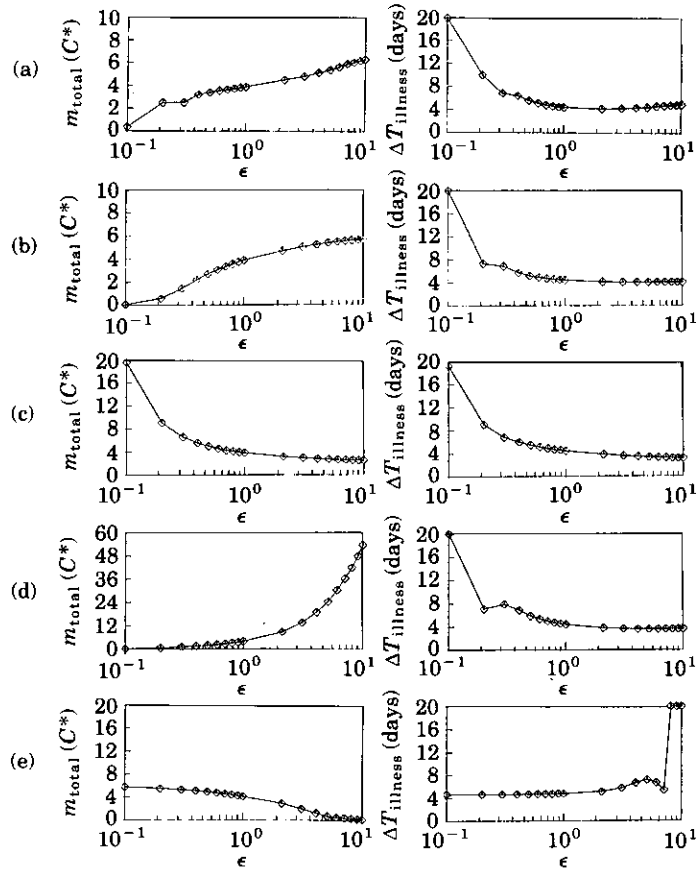

FIG. 7. Investigation of dependence on selected model parameters ν, σ, γ_{MV}, C^* and ρ_I of disease severity and duration characteristics, m_{total} and $\Delta T_{\text{illness}}$. The parameters are varied according to the relation $\alpha = \alpha^* \cdot \epsilon$, where α^* is the basic value of parameter α, given in Table 5 and $10^{-1} \leqslant \epsilon \leqslant 10$. The numerically calculated estimates of the characteristics over the interval 0–20 days are marked by squares. (a) influenza A virus replication rate (ν); (b) lung epithelial cells infection rate (σ); (c) macrophage stimulation rate (γ_{MV}); (d) amount of epithelial cells susceptible for influenza A virus infection (C^*); (e) rate of interferon secretion (ρ_I).

following: a simultaneous increase in H_E^* and H_B^* induces a fall in m_{total}, $m_{\max}$, $\Delta T_{\text{illness}}$, a rise in $P_{\max}$, P_{new} and a slight decrease in both, maximal and total numbers of CTLs generated by IAV driven clonal expansion. It should be noted that even a 100-fold drop in H_E^* and H_B^* doesn't lead to the virus persistence regime: the corresponding solutions mimic a complete elimination of viruses.

Changing IFN molecules secretion rate in the range $10^{-2} \leqslant (\rho_I/\rho_I^*) \leqslant 10^2$ revealed interesting consequences. Increasing values of ρ_I modify solution characteristics in such a way that both the total and maximal numbers of destroyed epithelial cells considerably decrease over a 0–20 day interval. However, starting from $\rho_I \sim 6 \times \rho_I^*$, the correlated drop in antigen level $V_{f_{\max}}$ results in insufficient antigenic stimulation of specific lymphocytes, manifested by a significant decrease of $E_{\max}$ and $P_{\max}$. Consequently IAV escapes from being controlled by the immune system. Thus, a virus persistence regime may be produced due to an IFN response which is not consistent with operating conditions of specific T and B cell clones. It is necessary to stress that IAV usually causes acute disease with a complete and rapid recovery. Nevertheless, persistence of IAV may occur in some individuals during interepidemic periods, and has been detected in the lungs of some human neonates and mice. Persistent infections with IAV have been established in cell lines and in organ cultures of human and other animal tissue. The mechanisms are not known, but in some cases persistence may have been mediated by IFN (Sweet & Smith, 1980).

The above results of parameterization of selected characteristics of the infection severity and duration and immune responsiveness we consider as first level proposals about the relationships between the course of influenza virus infection and host defense mechanisms.

7. Discussion

Mathematical modeling of infectious diseases on an individual level remains a relatively underexplored area despite its considerable theoretical importance.

We have presented an approach to an analysis and quantitative description of the organization and dynamic properties of basic defense processes developing in adult individuals during uncomplicated influenza A infection. The mathematical model of antiviral immune response, formulated within the Clonal Selection paradigm, was drawn on to organize existing knowledge about the variety of mechanisms contributing to influenza infection course over a 7 day interval. The model represents the infectious processes by thirteen state variables: influenza A viruses, infected epithelial cells, IFN-protected epithelial cells, destroyed epithelial cells, antigen-presenting macrophages, IFN-producing macrophages, interferon molecules, Th1 and Th2 helper cells, CTLs, B cells, plasma cells, and antibodies. For earlier quantitative mathematical models of antigen-driven clonal expansion see Bell, 1970; Bruni, *et al.*, 1978. Quantitative features of the immune response to growing antigen generated by immune networks have been studied theoretically by Rose & Perelson (1992).

The principal problem of our research was the lack of homogeneous data sets characterizing the infection in an individual in terms of the specific characteristics (model variables). To this end many different experimental facts and heterogeneous data from immunology, virology and clinical practice were generalized into an integrated and intuitively consistent quantitative sketch of the infection. The key aspect of the adjustment between the model and various data on the immune-specific and non-specific defense processes in influenza infection is the derivation of the generalized picture (GP) of uncomplicated IAV infection. This provides a holistic theoretical definition, in quantitative terms, of the kinetics of the normal or typical course of the disease and the antiviral immune response. The corresponding data set is as yet sparse but it is open for both constructive criticism and supplement, and should be considered as an intermediate level of data organization between incomplete experimental and clinical observations and a mathematical model of IAV infection.

The pragmatic aim of the GP is to assemble and represent the data necessary to refine estimates of the model parameters corresponding to IAV infection. Our approach to parametric analysis is based on taking into account the localization of immune response and disease variables to three different compartments—lung epithelium, lung associated lymphoid tissue and mucous, rather than considering the organism as a well-mixed homogeneous reactor.

The infection processes considered in the model are characterized by about 60 parameters. The parameter set of the model may be divided into two groups. The first consists of parameters for which direct estimates from reported observation data are available: the homeostatic proportions for major lymphocyte subsets, the half-life times of immune cells and immunoglobulins, the characteristics of division and differentiation processes of T and B cells, the rates of antibody production by plasma cells and viruses by infected cells and, so on. The second group is formed of parameters characterizing the rates of cell-to-cell interactions in virus-sensitive tissue and lymph nodes, for which no direct estimates are available. The results of parameter analysis of antiviral immune response during acute hepatitis B virus infection may be utilized to a certain degree for modeling IAV infection. As this takes place, clearly established specific features of influenza infection, such as the role of nonspecific mechanisms limiting the infection (IFN response, inflammatory response, etc), cross-reactivity phenomena, the secondary character of T cell response in adults, should be taken into account and corresponding corrections of parameter estimates are required. These include the higher frequencies of T and B cells specific for IAV antigens, a finer time scale while analyzing clone formation characteristics.

Initial estimates were made for all parameters. Those parameters that govern the kinetics of virus replication and infection of epithelial cells, antigen-presenting cells stimulation, were refined by fitting to the GP data for uncomplicated influenza. The final estimates characterize the intrinsic rates of immune mechanisms and infection processes. They make explicit the idea of an evolutionary established balance between immune responsiveness and IAVs for the human population.

The set of model parameters provides a single scale for comparing immune responses to different infectious agents. It is an interesting modeling result that two extreme viral challenges (IAV and HBV) may be neutralized by specific clone selection and activation processes which are characterized by the same rates of macrophage-lymphocyte and lymphocyte-lymphocyte interactions in the LN compartment. Thus, an invariant parametric kernel for the "immune" submodel of the mathematical model of antiviral immune response can be separated from the total set of parameters, characterizing the stereotypic component of immune responsiveness. The schematic model of the defense mechanisms, which provide protection of the host in IAV infection, considered in the basic model for specific components of antiviral immune response, is not complete. The model was extended to include a description of phagocyte-mediated inflammatory response, which supplements the cytotoxic

action of specific CTLs. In addition, in the case of IAV infection the interferon response was shown to play a vital role in limiting the spread of influenza virus during the initial phase of infection, before the specific components of the immune response are able to bring the infectious processes under control. The fast nonspecific IFN mechanism is required to compensate for the inertia of the clonal selection and activation processes. A similar function is performed by the inflammation process during bacterial infection.

Careful quantitative analysis of the IFN system, permitting evaluation of the IFN reaction parameters, was based upon the idea that tissue macrophages in the epithelium compartment are responsible for the majority of IFNα molecules, inducing an antiviral state of sensitive cells. We have shown that the antiviral immune response model may be extended to include explicitly the antiviral IFN response kinetics while keeping the core descriptive tool of the model—the particular set of parameter values.

Verification of the model was carried out by semi-quantitative simulations of the immune protection phenomena of susceptible individuals. It was found that a joint 50-fold increase in IAV specific Abs and CTL frequencies is sufficient to protect susceptible individuals against infection with realistic doses of IAV.

We consider our model to be a correct descriptive tool for short-range ($\sim$7 days) immune processes (limited to a number of clones) taking place during acute IAV infection diseases with complete and rapid recovery. In considering the limitations of our model the following points need to be mentioned:

- the unique CTL chain should be divided into proliferating and effector subsets (compare with the B cell and plasma cell subsets of the model) if the kinetics of CTLs in both LN and sensitive tissue compartments are to be described;
- the parameterization of the negative feedback function $\xi(m)$ in the model is not sufficiently supported by data;
- the processes of immune memory generation i.e. the later differentiation phases of immune response, should be incorporated into the model.

Persistent or latent infections, such as chronic hepatitis B or HIV infection (see recent studies of Mclean & Kirkwood, 1990; Nelson & Perelson, 1991; Nowak *et al.*, 1991) clearly require inclusion and formulation of long-range regulatory processes in the immune system rather than in separated clones only. This, however requires more rigorous elaboration of the notions of immune homeostasis and resources.

An analysis of the relative balance between different mechanisms that must operate *in vivo* to constitute a workable immune system revealed the equal importance of non-specific and specific immune mechanisms of virus neutralization in influenza. The role of immunopathology in influenza is considered to be minimal since the main clinical and pathological events happen quickly after the onset of infection. Indeed, the total number of infected epithelial cells destroyed by CTL turns out to be ten times less than that by direct cytopathic effects of IAVs (see Table 7). It seems interesting to note that the cumulative number of destroyed virus-sensitive cells turned out to be several times greater than the homeostatic size of the susceptible tissue, thus a burst of regeneration processes takes place during influenza.

The sensitivity analysis of the influenza model has revealed that virus and sensitive tissue characteristics exert primary control over the variations of the disease course, rather than immune responsiveness parameters. The results presented in Section 6 show that the severity of influenza is most sensitive to the parameters of the IAV—epithelial cell interactions, whereas the variations in the duration of illness are under the influence of humoral immune response parameters. The rate of antigen-driven clonal expansion is controlled by proliferation parameters and antigen-presenting cells activity decay. The latter correlates with the findings of Fishman & Perelson (1993) on the profound consequences of the life-time of the antigen-presenting state on the dynamics of T cell response.

Surprising was the remarkable sensitivity of the clonal expansion progression to the IAV replication rate. The sensitivity indices may be used as uncertainty measures for populational variations in the influenza course during epidemics. These characteristics of each individual's sensitivity to a variety of host–virus relationship factors need to be related to and interpreted using the population level data on IAV virulence and immune response heterogeneity to assess numerically the evolutionarily established equilibrium between infectious agents and immune system effectiveness. A parameter variation analysis suggests a prolonged persistence of the influenza virus in a host that can occur due to an imbalance between the rapid and non-specific IFN response and the more inertial and adaptive immune response. Thus, the normal immune system operates in such a way that the IFN response is kinetically adjusted with specific clonal expansion processes. These results together with our previous studies on the contribution of the immune system to protection and pathology of acute HBV infection may be useful in elaborating the notion of

optimal defense against viruses, as is currently used in the theoretical analysis of evolutionary relationships between viruses and immune system (Zinkernagel *et al.*, 1985; Doherty, 1985).

In many fields of pure and applied science the central issue is the determination of mathematical models that are consistent with both observations and prior knowledge. We have presented a multiparameter modeling approach for the theoretical study of the kinetic pattern of immune reaction *in vivo*, which is, however, a very crude representation of real complexity and fine tuning of immune processes (Perelson & Oster, 1979; Brendel & Perelson, 1987; Kauffmann *et al.*, 1988; Gandolfi & Strom, 1990; Stewart & Varela, 1991; De Boer *et al.*, 1992). Nevertheless, such studies may provide new guidelines and dimensions in the theoretical analysis of problem areas in interactions of viruses and immune system (Doherty, 1986).

Our approach to modeling is based on the use of delay equations. First, they may be considered as a natural way to represent a duration of lymphocyte's division and differentiation processes during the antiviral immune response. It means that the delays are directly measurable and explicitly controllable parameters (by steroid hormones, other intrinsic or external factors). The use of delay equations makes it possible to assess in an obvious way the quantities of dividing cells thus enabling a direct reference to experiments. Second, the severity and outcome of influenza infection result from the races over a few days between the viral spread in a sensitive tissue and the clonal expansion of specific lymphocytes. On a short-time scale (7 days) the delay equations (with the lags about 1 day) give a kinetics which is, in general, quantitatively different from that due to ODEs. For example, a solution to a simplest linear constant delay equation is represented by a polynomial in the independent variable t (El'sgolts & Norkin, 1973), rather than an exponential function, which is typical for a simplest scalar ordinary differential equation. Only for large time intervals as compared to the value of delay these types of behavior can converge. These two points were the basic reasons to consider explicitly the delays in the model equations. However, in future we will try to perform a separate research to clarify more rigorously and quantitatively the domains of the principle difference between modeling approaches based on DDEs and ODEs in the particular field of infectious disease studies.

A practically important aspect of influenza is that it promotes secondary bacterial infections that are sometimes fatal. A quantitative assessment by mathematical modeling of the underlying mechanisms of immunodeficiency and immunomodulation is an element of the groundwork for an exploration of risk factors that alter the course and outcome of influenza virus infections.

This research was partly supported by the Federal Department of Science (Russia) Grant 3.418.2 through its Informatization Program and by the International Science Foundation. The authors are indebted to Prof. G. I. Marchuk for scientific support. We thank Prof. E. B. Tozulahova for productive discussions on the interferon system. The authors are indebted to the Journal referees for their valuable comments which were very important in improving the presentation of the key aspects of our research.

REFERENCES

ADA, G. (1991). Strategies for exploiting the immune system in the design of vaccines. *Molec. Immun.* **28(3),** 225–230.

ADA, G. L. & JONES, P. D. (1986). The immune response to influenza infection. *Curr. Top. Microbiol. Immun.* **128,** 1–54.

ALLEN, R. C. & PRUESS, S. A. (1981). An analysis of an inverse problem in ordinary differential equations. *SIAM J. Sci. Statist. Comput.* **2,** 176–185.

BALKWILL, F. R. (1986*a*). Interferons: From molecular biology to man. Part 1. Genetics and molecular biology of the interferon system. *Microbiol. Sci.* **3(7),** 212–215.

BALKWILL, F. R. (1986*b*). Interferons: From molecular biology to man. Part 2. Interferons and cell function. *Microbiol. Sci.* **3(8),** 229–233.

BALKWILL, F. R. (1986*c*). Interferons: From molecular biology to man. Part 3. Interferons and disease. *Microbiol. Sci.* **3(9),** 281–284.

BARD, Y. (1974). *Nonlinear parameter estimation.* New York: Academic Press.

BARON, S., DIANZANI, F. & STATON, G. J. (1981). General considerations of the interferon system. *T. Rep. Biol. Med.* **41,** 1–12.

BEASLEY, R., ROCHE, W. R., ROBERTS, J. A. & HOLGATE, S. T. (1989). Cellular events in the bronchi in mild asthma and after bronchial provocation. *Am. Rev. Respir. Dis.* **139(3),** 806–817.

BELL, G. I. (1970). Mathematical model of clonal selection and antibody production. *J. theor. Biol.* **29,** 191–232.

BELOSO, A., MARTINEZ, C., VARCARCEL, J., SANTAREN, J. F. & ORTIN, J. (1992). Degradation of cellular mRNA during influenza virus infection: its possible role in protein synthesis shutoff. *J. Gen. Virol.* **73(3),** 575–581.

BOCCI, V. (1985). Distribution, catabolism and pharmacokinetics of interferon. In: *Interferon.* In vivo *and clinical studies,* Vol. 4 (Finter, N. B. & Oldham, R. K., eds) pp. 145–154. North Holland: Elsevier Science Publishers.

BOCHAROV, G. A. & ROMANYUKHA, A. A. (1990). Mathematical model of antiviral immune response during Influenza A virus infection. Dept. Num. Math., USSR Acad. Sci. Moscow: preprint N 271 (in Russian).

BOCHAROV, G. A. & ROMANYUKHA, A. A. (1994). Numerical treatment of parameter identification problems for delay-differential systems arising in immune response modeling. *Appl. Num. Math.* (in press).

BOGGS, P. T., BYRD, R. H. & SCHNABEL, R. B. (1987). A stable and efficient algorithm for nonlinear orthogonal distance regression. *SIAM J. Sci. Statist. Comput.* **8(6),** 1052–1078.

BORECKY, L., LACKOVIC, V., FUCHSBERGER, N. & HAJNICKA, V. (1974). Activation of macrophages (Wagner, W. & Hahn, H., eds), pp. 111–122. New York: Elsevier.

BORN, W. K., HARSHAN, K., MODLIN, R. L. & O'BRIEN, R. L. (1991). The role of $\gamma\delta$ T lymphocytes in infection. *Curr. opin. Immun.* **3(4),** 455–459.

BRAIN, J. D. (1970). Free cells in the lung. Some aspects of their role, quantitation, and regulation. *Arch. Intern. Med.* **126,** 477–487.

BRENDEL, V. & PERELSON, A.S. (1987). Kinetic analysis of absorption processes. *SIAM J. Appl. Math.* **47(6),** 1306–1319.

BRUNI, C., GIOVENCO, M. A., KOCH, G. & STROM, R. (1978). Modeling of the immune response: a system approach. In: *Theoretical Immunology* (Bell, G., Perelson, A. & Pimbley, G., eds), pp. 379–414. New York: Marcel Dekker.

CHONMAITREE, T., ROBERTS, N. J., DOUGLAS, R. G., HALL, C. B. & SIMONS, R. L. (1981). Interferon production by human mononuclear leukocytes: differences between respiratory syncytial virus and influenza viruses. *Infect. Immun.* **32,** 300–303.

CHONMAITREE, T., LETT-BROWN, M. A., TSONG, Y. I., GOLDMAN, A. S. & BARON, S. (1988). Role of interferon in leukocyte histamine release caused by common respiratory viruses. *J. Infect. Dis.* **157(1),** 127–132.

CLARKE, S. W. (1983). Physical defenses of the respiratory tract. *Eur. J. Respir. Dis.* (Suppl.) 126, 64. 27–30.

COUCH, R. B. & KASEL, J. A. (1983). Immunity to influenza in man. *Ann. Rev. Microbiol.* **37,** 529–549.

DE BOER, R. J. & PERELSON, A. S. (1991). Size and Connectivity as Emergent Properties of a Developing Immune Network. *J. theor. Biol.* **149,** 381–424.

DE BOER, R. J., VAN DER LAAN, J. D. & HOGEWEG, P. (1992). Randomness and pattern scale in the immune network. A cellular automata approach. In: *Thinking About Biology, SFI Lectures in Complex System.* (Varela, F. J. & Stein, W. D., eds), Redwood City, CA: Addison-Wesley.

DE BOER, R. J., KEVREKIDIS, I. G. & PERELSON A. S. (1993*a*). Immune network behaviour. I. From stationary states to limit cycle oscillations. *Bull. Math. Biol.* **55,** 745–780.

DE BOER, R. J., KEVREKIDIS, I. G. & PERELSON, A. S. (1993*b*). Immune network behavior. II. From oscillations to chaos and stationary states. *Bull. Math. Biol.* **55,** 781–816.

DEPPER, J. M., LEONARD, W. J., KRONKE, M., NOGUCHI, P. D., CUNNINGHAM, R. E., WALDMANN, T. A. & GREENE, W. C. (1984). Regulation of interleukin 2 receptor expression: effects of phorbol diester, phospholipase C, and reexposure to lectin or antigen. *J. Immun.* **133(6),** 3054–3061.

DIANZANI, F., VIANO, I., SANTIANO, M., ZUCCA, M., GULLINO, P. & BARON, S. (1978). Tissue culture models of *in vivo* interferon production and action. In: *Human Interferon. Production and Clinical Use. Adv. Exp. Med. Biol.* Vol. 110, (Stinebring, W. R. & Chapple P. U., eds), pp. 119–131. New York: Plenum.

DIANZANI, F. & BARON, S. (1984). Cell products antagonizing viral infections in tissues: interferon and other nonspecific inhibitors. In: *Bacterial and Viral Inhibition and Modulation of Host Defences* (Falkone G., ed.) pp. 41–60. London: Academic Press.

DOHERTY, P.C. (1985). T cells and viral infections. *Br. Med. Bull.* **41(1),** 7–14.

DOHERTY, P. C. (1986). Some problem areas in the interaction between viruses and the immune system. *Immun. Cell. Biol.* **65,** 279–286.

DONGARRA, J. J., BUNCH, J. R., MOLER C. B. & STEWART G. W. (1979). *LINPACK Users Guide.* Soc. Ind. Appl. Math. Philadephia.

EL'SGOLTS, L. E. & NORKIN, S. B. (1973). *Introduction to the Theory and Applications of Functional Differential Equations with Deviating Arguments.* New York: Academic Press.

FEDOSEEV, G. B. & GEHAREV, S. S. (1989). Basic defense mechanisms of bronchio-lung system. In: *General Pulmonology*, Vol. 1 (Putov, N. V., ed.), pp. 112–144. Moscow: Medicina (in Russian).

FIELDS, B. N. & KNIPE, D. M. (eds) (1986). *Fundamental Virology.* New York: Raven Press.

FISHMAN, M. A. & PERELSON, A. S. (1993). Modeling T Cell-Antigen Presenting Cell Interactions. *J. theor. Biol.* **160,** 311–342.

GANDOLFI, A. & STROM, R. (1990). Cell-mediated antigen presentation to T_H cells: mathematical model. *IASI (CNR)* R. No. 315, Rome.

GOREN, T., FISCHER, D. G. & RUBINSTEIN, M. (1986). Human monocytes and lymphocytes produce different mixtures of α-Interferon subtypes. *J. Interferon Res.* **6,** 323–329.

HARRIS, R. E. (1984). Influenza during pregnancy. In: *Virus Infection in Pregnancy.* (Amstey, M. S., ed.), pp. 35–51. Orlando, FL: Grune and Stratton.

HEINO, M., JUNTUNEN-BACKMAN, K., LEIJALA, M., RAPOLA, J. & LAITINEN, L. A. (1990). Bronchial epithelial inflammation in children with chronic cough after early lower respiratory tract illness. *Am. Rev. Respir. Dis.* **141,** 428–432.

HIGHAM, D. J. & HIGHAM, N. J. (1991). Componentwise perturbation theory for linear systems with multiple right-hand side. Numerical Analysis Report N.200. University of Manchester.

HIMMELBLAU, D. M., JONES, C. R. & BISCHOFF, K. B. (1967). Determination of rate constants for complex kinetics models. *Ind. Eng. Chem. Fund.* **6(4),** 539–543.

HOFMAN, F. M., MODLIN, R. L., BHOOPAT, L. & TAYLOR, C. R. (1985). Distribution of cells bearing the Tac antigen during ontogeny of human lymphoid tissue. *J. Immun.* **134(6),** 3751–3755.

HOLT, P. G., SCHON-HEGRAD, M. A. (1987). Localization of T cells, macrophages and dendritic cells in rat respiratory tract tissue: implications for immune studies. *Immunology* **62,** 349–356.

HOSTEN, L. H. (1979). A comparative study of short cut procedures for parameter estimation in differential equations. *Comp. Chem. Eng.* **3,** 117–126.

IMSL (1980). *IMSL Library Reference Manual* 1–3. Houston: IMSL.

ISAACS, A. & LINDENMANN, J. (1957). Virus interference: I. The interferon. *Proc. R. Soc. Lond.* **B147,** 258–263.

JACKSON, G. G. & MULDOON, R. L. (1975). Viruses causing common respiratory infections in man. V. Influenza A (Asian). *J. Infect. Dis.* **131(3),** 308–357.

JAKAB, G. J. (1990). Sequential virus infections, bacterial superinfections, and fibrogenesis. *Am. Rev. Respir. Dis.* **142,** 374–379.

JANEWAY, C. A. JR (1988). Frontiers of the immune system. *Nature, Lond.* **333,** 804–806.

JANEWAY, C. A. JR (1992). The immune system evolved to discriminate infectious nonself from noninfectious self. *Immun. Today,* **13(1),** 11–16.

JOKLIK, W. K. (1985). Interferons. In: *Virology* (Fields, B. N., Knipe, D. M., Melnick, J. L., Chanock, R. M., Roizman, B., Shope, R. E., eds), pp. 281–307. New York: Raven Press.

KARPOV, A. V. (1992). Mathematical modeling of immune response during destructive pneumonia. Ph.D. Thesis. Institute of Numerical Mathematics, Moscow. (In Russian).

KAUFFMAN, S. A., WEINBERGER, E. D. & PERELSON, A. S. (1988). Maturation of the immune response via adaptive walks on affinity landscapes. In: *Theoretical Immunology Part I* (Perelson, A. S., ed.), pp. 349–382. Reading, MA: Addison-Wesley.

KEENAN, K. P., COMBS, J. W. & MCDOWELL, E. M. (1982*a*). Regeneration of hamster tracheal epithelium after mechanical injury. I. Focal lesions: Quantitative morphologic study of cell proliferation. *Virchows. Arch.* **B41,** 193–214.

KEENAN, K. P., COMBS, J. W. & MCDOWELL, E. M. (1982*b*). Regeneration of hamster tracheal epithelium after mechanical injury. II. Multifocal lesions: Stathmokinetic and autoradiographic studies of cell proliferation. *Virchows. Arch.* **B41,** 215–229.

KILBURNE, E. D. (1987). Influenza in man. In: *Influenza* (Kilburne, E. D., ed.) pp. 157–218. New York: Plenum.

KINGSBURY, D. W. (1986). Orto- and paramyxoviruses replication. In: *Fundamental Virology.* Vol. 2 (Fields, B. N. & Knipe, D. M., eds), pp. 446–486. New York: Raven Press. (Russian transl.)

KOZAK, M. (1986). Regulation of protein synthesis in virus-infected animal cells. *Adv. Virus Res.* **31,** 229–292.

LEIGH, M. W., CARSON, J. L. & DENNY, F. W. JR (1991). Pathogenesis of respiratory infections due to influenza virus: implications for developing countries. *Rev. Infect. Dis.* **13,** (Suppl. 6), 5501–5508.

LECHNER, J. F., HANGEN, A., MCCLENDON, I. A. & PETTIS, E. W. (1982). Clonal growth of normal adult human bronchial epithelial cells in serum-free medium. *In Vitro*, **18(7)**, 633–642.

LURIA, S. E., DARNELL, J. E. JR., BALTIMORE, D. & CAMPBELL, A. (1978). *General Virology*, 3rd edn. New York: John Wiley & Sons.

MARCHUK, G. I. & PETROV, R. V. (1983). Viral damage of sensitive tissue and immunophysiological defense reactions. (Mathematical model). Moscow, Inst. Num. Math. Acad. Sci. Moscow, pre-print. N.51 (in Russian).

MARCHUK, G. I. & BERBENTZOVA, A. P. (1989). Acute pneumonia: immunology, severity estimation, clinics and treatment. Moscow: Nauka (in Russian).

MARCHUK, G. I., PETROV, R. V., ROMANYUKHA, A. A. & BOCHAROV, G. A. (1991*a*). Mathematical model of antiviral immune response. I. Data analysis, generalized picture construction and parameters evaluation for hepatitis B. *J. theor. Biol.* **151**, 1–40.

MARCHUK, G. I., ROMANYUKHA, A. A., BOCHAROV, G. A. (1991*b*). Mathematical model of antiviral immune response. II. Parameters identification for acute viral hepatitis B. *J. theor. Biol.* **151**, 41–70.

MARCUS, P. I. (1983). Interferon induction by viruses. In: *Interferon*, Vol. 5. (Gresser, I., ed.). New York: Academic Press.

MARTZ, E., HEAGY, W. & GROKOWSKI, S. H. (1983). The mechanism of CTL-mediated killing: monoclonal antibody analysis of the roles of killer and target-cell membrane proteins. *Immun. Rev.* **72**, 73–96.

MCLAREN, C., GRUBBS, G. E. & ENNIS, E. A. (1978). Detection of cells producing surface antigen-specific antibody to influenza viruses. *J. Clin. Microbiol.* **8(4)**, 438–444.

MCLEAN, A. R. & KIRKWOOD, T. B. L. (1990). A model of HIV infection in T helper cell clones. *J. theor. Biol.* **147**, 177–203.

MITCHELL, D. M., MCMICHAEL, A. J. & LAMB, J. R. (1985). The immunology of influenza. *Br. Med. Bull.* **41**, 80–85.

MOGENSEN, S. C. & VIRELIZIER, J.-L. (1987). The interferon-macrophage alliance. In: *Interferon*, Vol. 8, (Gresser, I., ed.), pp. 58–84. London: Academic Press.

MOSIER, D. E. (1986). T cell activation of antigen-specific antibody responses by large B cells is MHC restricted. *J. Immun.* **136(6)**, 2090–2094.

MURPHY, B. R. & WEBSTER, R. G. (1985). Influenza viruses. In: *Virology*, (Fields, B. N., Knipe, D. M., Melnick, J. L., Chanock, R. M., Roizman, B. & Shope, R. E., eds), pp. 1179–1239. New York: Raven Press.

MURPHY, B. R., NELSON, D. L., WRIGHT, P. F., TIERNEY, E. L., PHELAN, M. A. & CHANOCK, R. M. (1982). Secretory and systemic immunological response in children infected with live attenuated influenza A virus vaccines. *Infect. Immun.* **36(3)**, 1102–1108.

NELSON, G. W. & PERELSON, A. S. (1991). A Mechanism of Immune Escape by Slow-Replicating HIV strains. Preprint 91-10-039, Santa Fe Institute. *J. AIDS* (in press).

NEWHOUSE, M., SANCHIS, J. & BIENENSTOCK, J. (1976). Lung defense mechanisms. *N. Engl. J. Med.* **295(18)**, 990–998.

NIEUWENHUIS, P. & OPSTELTEN, D. (1984). Functional anatomy of germinal centers. *Am. J. Anat.* **170**, 421–435.

NOWAK, M. A., ANDERSON, R. M., MCLEAN, A. R., WOLFS, T. F. W., GOUDSMIT, J. & MAY, R. M. (1991). Antigenic diversity thresholds and the development of AIDS. *Science* **254(5034)**, 963–969.

PAUL, W. E. (ed.) (1984). *Fundamental Immunology*. New York: Raven Press.

PAUL, W. E. (1987). Between two centures: Specificity and regulation in immunology. *J. Immun.* **139(1)**, 1–6.

PERELSON, A. S. & OSTER, G. F. (1979). Theoretical studies of clonal selection: minimal antibody repertoire size and reliability of self–non-self discrimination. *J. theor. Biol.* **81**, 645–670.

PERELSON, A. S. & BELL, G. I. (1982). Delivery of lethal hits by cytotoxic T lymphocytes in multicellular conjugates occurs in sequentially but at random times. *J. Immun.* **129**, 2796–2801.

PERELSON, A. S. (1988). Towards a realistic model of the immune network. In: *Theoretical Immunology Part Two, SFI Studies in the Science of Complexity*, Vol. III. (Perelson, A. S., ed.), pp. 337–401. Redwood, CA: Addison-Wesley.

PERELSON, A. S. & WEISBUCH, G. (1992). Modeling immune reactivity in secondary lymphoid organs. *Bull. Math. Biol.* **54**, 649–672.

POLIAK, B. T. (1983). Introduction into optimization. Moscow: Nauka (in Russian).

REYNOLDS, H. Y. & NEWBALL, H. H. (1976). Fluid and cellular milieu of the human respiratory tract. In: *Immunologic and Infectious Reactions in the Lung* (Kirkpatrick, C. H. & Reynolds, H. Y., eds), pp. 3–27. New York: Marcel Dekker.

REYNOLDS, H. Y (1989). Normal and defective respiratory host defenses. In: *Respiratory Infections: Diagnosis and Management*, 2nd edn (Pennington, J. F., ed.), pp. 1–33. New York: Raven Press.

RICHTMYER, R. D. (1978). *Principles of Advanced Mathematical Physics*, Vol. 1. New York: Springer-Verlag.

ROBERTS, N. J. JR., DOUGLUS, R. G. JR., SIMONS, R. M. & DIAMOND, M. E. (1979). Virus-induced interferon production by human macrophages. *J. Immun.* **123(1)**, 365–369.

ROMANYUKHA, A. A., BOCHAROV, G. A., MARCHUK, G. I. (1992). Mathematical modeling of infectious diseases. In: *Mathematical Aspects of Human Diseases, Applied Mathematics Monographs, CNR.* (Da Prato, G., ed.). Vol. 3, pp. 126–148. W Pisa: Giardini Editori E Stampatori.

ROSE, R. & PERELSON, A. S. (1992). Immune Networks and Immune Responses. Preprint 92-12-058. Santa Fe Institute. *Lect. Notes Biomath.*, Vol. 100 (Levin, S., ed.). Berlin: Springer-Verlag (in press).

RUSZNYAK, J., FOLDI M. & SZABO, G. (1957). *Physiology and Pathology of Lymphocirculation.* Budapest: Acad. of Sci. (in Russian).

SAPIN, M. R. & BORZIAK, E. I. (1982) *Extracorporal lymphatic transport pathways*. Moscow: Medicina (in Russian).

SAPIN, M. R., YURINA, N. A. & ETINGEN, L. E. (1978). *Lymph node.* Moscow: Medicina (in Russian).

SCOTT, G. M. (1984). How do viruses overcome mucosal defences? In: *Bacterial and Viral Inhibition and Modulation of Host Defences* pp. 25–39. London: Academic Press.

SEGEL, L. A. & PERELSON, A. S. (1989). Shape-space: an approach to the evaluation of cross-reactivity effects, stability and controllability in the immune system. *Immun. Lett.* **22**, 91–100.

SEMENOV, B. F., CAULEN, D. R. & BALANDIN, I. G. (1982). *Cellular and Molecular Basis of Antiviral Immunity*. Moscow: Medicina (in Russian).

SENGBUSCH, P. (1979). *Molecular and Cellular Biology*. Berlin: Springer-Verlag.

SHEVACH, E. M. (1984). Macrophages and other accessory cells. In: *Fundamental Immunology*. (Paul, W. E., ed.), pp. 71–107. New York: Raven Press.

SHWARTZMAN, I. S. & CHAZENSON, L. B. (1978). *Local immunity*. Leningrad: Medicina. (in Russian).

SIDOROV, I. A. & ROMANYUKHA, A. A. (1993). Mathematical modeling of T cell proliferation process. *Math. Biosci.* **115**, 187–232.

STEWART II, W. E. (1986). Interferons and their roles in virus infections. In: *Viruses, Immunity, and Immunodeficiency* (Szentivanyi, A. & Freidman, H., eds), pp. 301–306. New York: Plenum Press.

STEWART, J. & VARELA, F. J. (1990). Dynamics of class of immune networks. II. Oscillatory activity of cellular and humoral components. *J. theor. Biol.* **144**, 103–115.

STEWART, J. & VARELA, F. J. (1991). Morphogenesis in shape-space. Elementary meta-dynamics in a model of the immune network. *J. theor. Biol.* **153**, 477–498.

SULLIVAN, K. M., MONTO, A. S. & FOSTER, D. A. (1990). Antibody response to inactivated influenza vaccines of various antigenic concentrations. *J. Infect. Dis.* **161**, 333–335.

SWEET, C. & SMITH, H. (1980). Pathogenicity of Influenza Virus. *Microbiol. Rev.* **44(2)**, 303–330.

TINSLEY, C. M., SWEET, C., COATES, D. M. & SMITH, H. (1987). The local origin of fever in influenza: differential production of endogenous oxygen by nasal inflammatory cells of ferrets exhibiting different levels of fever. *FEMS Microbiol. Lett.* **42(2–3)**, 103–108.

TOEWS, G. B. (1989). Pulmonary clearance of infectious agents. In: *Respiratory Infections: Diagnosis and Management*, 2nd edn. (Pennington, J. F., ed.), pp. 41–51. New York: Raven Press.

TUKEY, J. W. (1977). *Exploratory Data Analysis*. Menlo Park, CA: Addison-Wesley.

TYRRELL, D. A. J. (1980). Vaccination. Influenza vaccines. *Phil. Trans. R. Soc. Lond.* **B288,** 449–460.

VARAH, J. M. (1982). A spline least squares method for numerical parameter estimation in differential equations. *SIAM J. Sci. Stat. Comput.* **3(1),** 28–46.

VLADIMIROV, N. S. (1988). *Mathematical Physics Equations*. Moscow: Nauka (in Russian).

WEIBEL, E. R. (1986). Functional morphology of lung parenchyma. In: *Handbook of Physiology, Section* 3: *The Respiratory System*, Vol. III: *Mechanics of Breathing*, (McKlem, P. T., ed.). Part 1, Chapter 8, pp. 89–111. J. Mead.

WEISBUCH, G. (1990). A shape space approach to the dynamics of the immune system. *J. theor. Biol.* **143,** 507–522.

WEISBUCH, G., DE BOER, R. J. & PERELSON, A. S. (1990). Localized memories in idiotypic networks. *J. theor. Biol.* **146,** 483–499.

WELLIVER, R. C. & OGRA, P. L. (1988). Immunology of respiratory viral infections. *Ann. Rev. Med.* **39,** 147–162.

WOHLFART, C. (1988). Neutralization of adenoviruses: kinetics, stoichiometry, and mechanisms. *J. Virol.* **62(7),** 2321–2328.

YERMAKOVA, A., VALKO, P. & VAJDA, S. (1982). Direct integral method via spline-approximation for estimating rate constants. *Appl. Catal.* **2,** 139–154.

ZDANOV, V. M. & BUKRINSKAJA, A. G. (1969). *Myxoviruses Reproduction*. Moscow: Medicina (in Russian).

ZINKERNAGEL, R. M., HENGARTNER, H. & STITZ, L. (1985). On the role of viruses in the evolution of immune responses. *Br. Med. Bull.* **41(1),** 92–97.

APPENDIX

Fitting of model to data

The problem of quantitative description by mathematical model of any data characterizing an object, without *a priori* suggestions on its stochastic nature, is considered as fitting of model parameters to data (Bard, 1974; Poliak, 1983), i.e. determining parameter's values giving the minimal deviation between model and data. The objective functional should be selected with the nature of both the observation data and nonlinearities generated by mathematical model taken into account (Tukey, 1977).

FITNESS MEASURING OBJECTIVE FUNCTIONAL: NATURE OF OBSERVATION DATA

In the classical least sqaures (LS) approach, model parameter values are selected by minimizing the sum of squared residuals, i.e. the objective functional has the structure

$$\Phi(\alpha) \sim \sum_{j=1}^{M} (y(t_j,\alpha) - y_{\text{obs}j})^2.$$

Here, $y_{\text{obs}j}$ stands for empirical data and $y(t_j,\alpha)$ are the model predictions at t_j. The limitations of classical LS approach to parameter optimization have been observed in several applications. For example, in curve fitting problems (Boggs *et al.*, 1987) it was pointed out that it unduly weights the top data points. This aspect of residual LS approach becomes critical in our applications, where typical sets of empirical data are characterized by large variations in absolute values over the observation interval and by equal significance of the data points independently of their absolute values. To measure the goodness of fit between model and data we consider the relative distances between observations and model predictions in terms of ratios

$$\frac{y_{\text{obs}j}}{y(t_j,\alpha)} \text{ and } \frac{y(t_j,\alpha)}{y_{\text{obs}j}},$$

rather than the residuals, $(y_{\text{obs}j} - y(t_j,\alpha))$. Thus, we take

$$\Phi(\alpha) \sim \sum_{j=1}^{M} F^2\{(y(t_j,\alpha), y_{\text{obs}j})\},$$

where $F(\cdot)$ meets the symmetry condition: $F(y_{\text{obs}}, y(\alpha)) = F(y(\alpha), y_{\text{obs}})$. The functional $\Phi(\alpha)$ employed in a previous work (Marchuk *et al.*, 1991*b*) had the following form:

$$\Phi(\alpha) = \sum_{j=1}^{M} \sum_{i=1}^{N} \left[\left(\frac{y^{(i)}(t_j,\alpha) - y^{(i)}_{\text{obs}j}}{y^{(i)}_{\text{obs}j}} \right)^2 + \left(\frac{y^{(i)}(t_j,\alpha) - y^{(i)}_{\text{obs}j}}{y^{(i)}(t_j,\alpha)} \right)^2 \right],$$

where observation data for the i-th model variable at time t_j are denoted by $y^{(i)}_{\text{obs}j}$ and corresponding model prediction by $y^{(i)}(t_j,\alpha)$; M is the total number of different observations times, N is the dimension of model state vector; α is the vector of identified parameters.

Another fitness functions for the relative deviations can also be used:

$$\Phi(\alpha) = \sum_{j=1}^{M} \sum_{i=1}^{N} \left[\left(\frac{y_{\text{obs}\,j}^{(i)}}{y^{(i)}(t_j, \alpha)} \right)^2 + \left(\frac{y^{(i)}(t_j, \alpha)}{y_{\text{obs}\,j}^{(i)}} \right)^2 \right], \quad \Phi(\alpha) = \sum_{j=1}^{M} \sum_{i=1}^{N} \left[\log \left(\frac{y_{\text{obs}\,j}^{(i)}}{y^{(i)}(t_j, \alpha)} \right) \right]^2.$$

The latter was applied for fitting a similar, antibacterial immune response model by Karpov (1992).

NONLINEARITY OF MODEL PREDICTIONS

Only for regression models, which are linear in their parameters, does the residual LS approach generate a linear LS problem. When the predictions are governed by differential models rather than algebraic, then the LS approach, even for linear models, generally leads to a nonlinear minimization problem. The nonlinearity of the fitness function $\Phi(\alpha)$ with respect to α results from a combination of the quadratic transformation $[\cdot]^2$, the ratios scaling function $F(\cdot)$ and the solution function $y(t, \alpha)$ of mathematical model formulated as a parameter-dependent differential system. The latter is characterized by exponential nonlinearities in t and α, at least locally. To decrease the nonlinearity of $\Phi(\alpha)$ the function F should be selected with this behavior of $y(t, \alpha)$ in mind.

To illustrate the idea, we consider the simplest case of the linear ODE model: $y' = \alpha \times y$. Let the model be exactly related to the observed process, and let α^* be the "true" parameter i.e. observations are described by $y_{\text{obs}}(t) = y_0 e^{\alpha^* t}$. The solution of the model for a perturbed α value with the given initial condition $y(0) = y_0$ is $y_0 e^{\alpha t}$. Then the classical residual LS approach leads to the nonlinear minimization problem for α:

$$\Phi(\alpha) \sim \sum_{j=1}^{M} (e^{\alpha t_j} - e^{\alpha^* t_j})^2 \to \min,$$

whereas the relative distance LS approach results in the problem:

$$\Phi(\alpha) \sim \sum_{j=1}^{M} (e^{(\alpha - \alpha^*) t_j})^2 \to \min$$

over $\Delta\alpha$. Selecting the scaling function $F(\cdot)$ as the logarithm, one decreases the exponential nonlinearity of model predictions with respect to α. This straightens out the behavior of y and y_{obs} with respect to α and t in the LS functional. With this choice, one arrives at the following minimization problem over $\Delta\alpha$:

$$\Phi(\alpha) \sim \sum_{j=1}^{M} (\alpha - \alpha^*)^2 t_j^2 \to \min.$$

The last formulation is the common linear LS problem corresponding to linear ODE model.

The real situations are much more complicated due to inexactness of the models, non-linearity of the differential system, noisy observation data, and non-exponential behavior of the solution in the "large". Nevertheless, the LS criterion for relative distances scaled by logarithmic transformation,

$$\Phi(\alpha) = \sum_{j=1}^{M} \sum_{i=1}^{N} w_{ji} \left[\log \left(\frac{y_{\text{obs}\,j}^{(i)}}{y^{(i)}(t_j, \alpha)} \right) \right]^2,$$

where w_{ji} represent the data weighting procedure, seems to be a good candidate for fitting problems in acute infection modeling.

This set of fitting problems is characterized by observation data which vary considerably in time in their magnitude, and predictions which represent evolutionary processes governed by ODE models. The observation (fitting) time interval should be subdivided into subintervals of clear exponential dynamic, each governed by a minimal number of processes, in order to make the corresponding minimization problem to be minimally non-linear.

PARAMETER REFINEMENT PROCEDURES

In a previous work (Marchuk *et al.*, 1991*b*) an approach to parameter refinement was suggested, which is characterized by splitting the optimization problem for model predictions on the complete observation interval into a set of optimization subproblems on smaller time intervals. This decomposition is developed using available qualitative information on the natural history of particular infectious diseases to choose a small number of optimized parameters, specifically for every subproblem. The parameters are considered to govern the kinetics of the observation data within corresponding subintervals. For details of the sequential refinement procedures,

see Bocharov & Romanyukha (1993). Parameter identification problems for the antiviral immune response model are huge and computationally expensive due to nonlinear (bi- and tri-linear) terms in right-hand sides of differential equations, non-monotone functions for initial conditions, high dimensionality and delays. To facilitate the solution of the basic constrained minimization problem:

$$\alpha^* = \arg(\min\Phi(\alpha))\ A \leqslant \alpha \leqslant B,$$

it is desirable to have a good (close to α^*) initial guess for parameter values, α_0.

Himmelblau *et al.* (1967) had proposed simplified methods for solution of inverse problems in chemical kinetics. These employ the idea of using observation data to generate spline-functions fitted to the model differential system, to avoid repeated solving of initial value problems for the differential system. By this means, instead of a nonlinear optimization problem for objective functional determined by differential system, a simpler LS problem for linear or nonlinear algebraic system is formulated. The approach suggested by Himmelblau and developed later by Allen & Pruess (1981), Varah (1982), Yermakova *et al.* (1982), Higham & Higham (1991), was further generalized to include typical situations in infectious disease modeling, when the observation data are available only for some of the state variables and the equations for the other variables can not be solved by quadratures.

The approach elaborated to model fitting essentially speeds up the treating of parameter identification problems. In general, it leads to non-unique parameter estimates or may be ill-conditioned. However, it allows more effective allocation of the process of model fitting to data between crude but simple and finer but computationally expensive methods. The corresponding code, suitable for fitting of delay-differential models to data, uses the standard algorithms of one-dimensional quasi-cubic interpolation based on Hermite polynomials IQHSCU (IMSL, 1980), the one dimensional quadrature adaptive procedure DCADRE (IMSL, 1980), the LINPACK algorithm for linear least squares problems, and the quasi-Newton method for nonlinear function minimization ZXMIN (IMSL, 1980).